



HAL
open science

A Catalog of Merging Dwarf Galaxies in the Local Universe

Sanjaya Paudel, Rory Smith, Suk Jin Yoon, Paula Calderón-Castillo,
Pierre-Alain Duc

► **To cite this version:**

Sanjaya Paudel, Rory Smith, Suk Jin Yoon, Paula Calderón-Castillo, Pierre-Alain Duc. A Catalog of Merging Dwarf Galaxies in the Local Universe. *The Astrophysical Journal Supplement*, 2018, 237 (2), pp.36. 10.3847/1538-4365/aad555 . hal-02373398

HAL Id: hal-02373398

<https://hal.science/hal-02373398v1>

Submitted on 6 Jan 2025

HAL is a multi-disciplinary open access archive for the deposit and dissemination of scientific research documents, whether they are published or not. The documents may come from teaching and research institutions in France or abroad, or from public or private research centers.

L'archive ouverte pluridisciplinaire **HAL**, est destinée au dépôt et à la diffusion de documents scientifiques de niveau recherche, publiés ou non, émanant des établissements d'enseignement et de recherche français ou étrangers, des laboratoires publics ou privés.

A CATALOG OF MERGING DWARF GALAXIES IN THE LOCAL UNIVERSE

SANJAYA PAUDEL,¹ RORY SMITH,² SUK JIN YOON,¹ PAULA CALDERÓN-CASTILLO,³ AND PIERRE-ALAIN DUC⁴

¹*Department of Astronomy and Center for Galaxy Evolution Research, Yonsei University, Seoul 03722, Korea*

²*Korea Astronomy and Space Science Institute, Daejeon 305-348, Republic of Korea*

³*Astronomy Department, Universidad de Concepción, Casilla 160-C, Concepción, Chile*

⁴*Université de Strasbourg, CNRS, Observatoire astronomique de Strasbourg, UMR 7550, F-67000 Strasbourg, France*

(Received July 20, 2018; Revised July 20, 2018; Accepted July 20, 2018)

Submitted to ApJS

ABSTRACT

We present the largest publicly available catalog of interacting dwarf galaxies. It includes 177 nearby merging dwarf galaxies of stellar mass $M_* < 10^{10} M_\odot$ and redshifts $z < 0.02$. These galaxies are selected by visual inspection of publicly available archival imaging from two wide-field optical surveys (SDSS III and the Legacy Survey), and they possess low surface brightness features that are likely the result of an interaction between dwarf galaxies. We list UV and optical photometric data which we use to estimate stellar masses and star formation rates. So far, the study of interacting dwarf galaxies has largely been done on an individual basis, and lacks a sufficiently large catalog to give statistics on the properties of interacting dwarf galaxies, and their role in the evolution of low mass galaxies. We expect that this public catalog can be used as a reference sample to investigate the effects of the tidal interaction on the evolution of star-formation, morphology/structure of dwarf galaxies.

Our sample is overwhelmingly dominated by star-forming galaxies, and they are generally found significantly below the red-sequence in the color-magnitude relation. The number of early-type galaxies is only 3 out of 177. We classify them, according to observed low surface brightness features, into various categories including shells, stellar streams, loops, antennae or simply interacting. We find that dwarf-dwarf interactions tend to prefer the low density environment. Only 41 out of the 177 candidate dwarf-dwarf interaction systems have giant neighbors within a sky projected distance of 700 kpc and a line of sight radial velocity range ± 700 km/s and, compared to the LMC-SMC, they are generally located at much larger sky-projected distances from their nearest giant neighbor.

Keywords: galaxies: dwarf, galaxies: evolution galaxies: formation - galaxies: stellar population

1. INTRODUCTION

A plethora of observational studies now support the conclusion that mergers between galaxies are frequent phenomena. In the Λ CDM cosmology (Spergel et al. 2007), the assembly of large scale structure happens in a hierarchical fashion, and mergers play a fundamental role in both the growth and evolution of galaxies (Conselice et al. 2009). Both observations and numerical simulations concur that massive elliptical galaxies were likely formed predominantly by the mergers of disk

galaxies (Springel et al. 2005; Naab et al. 2007; Duc et al. 2011, 2015).

On the other hand, it is a common belief that the shallow potential well of low mass galaxies causes them to be more sensitive to their surrounding environment than massive galaxies. Dwarf galaxies exhibit a strong morphological segregation: the most evolved / oldest dwarf galaxies (i.e dwarf Spheroidal (dSph) or dwarf early-type (dE)) are found exclusively in the group and cluster environments (Kormendy et al. 2009; Lisker 2009; Boselli & Gavazzi 2006). Meanwhile dwarfs with ongoing star-formation activity (such as Blue Compact Dwarf galaxies (BCDs, Gil de Paz et al. 2003; Papaderos et al. 1996) or dwarf irregulars (dIrs, Gallagher et al. 1984) are mainly found in less dense environments. Indeed, a study of the environmental dependence on the star-formation activity in dwarf galaxies by Geha et al. (2012) concluded that early-type dwarf galaxies ($10^6 <$

sanjpaudel@gmail.com (SP)
rorysmith@kasi.re.kr (RS)
sjyoon0691@yonsei.ac.kr (SJY)
ashniet.caskortish@gmail.com (PCC)
pierre-alain.duc@astro.unistra.fr (PAD)

$M_* < 10^9$) are extremely rare in the field. The origin of the different dwarf galaxy types and the possible evolutionary links between them are the subject of much research and debate (Lisker 2009).

The evolution of dwarf galaxies throughout the merging process has yet to be explored in detail. However, in the last few years the observational evidence for mergers between dwarf galaxies has been growing (e.g. Amorisco et al. 2014; Crnojević et al. 2014; Martínez-Delgado et al. 2012; Johnson 2013; Nidever et al. 2013; Rich et al. 2012; Paudel et al. 2017). The possibilities that certain low mass early-type galaxy (or dEs) might also be formed through mergers, similar to massive ellipticals, has been speculated in order to explain peculiar observational properties such as kinematically decoupled cores and boxy shape isophotes (Toloba et al. 2014; Graham et al. 2012; Geha et al. 2005). If this is the case, one might expect the progenitors of some dEs to exhibit characteristic features that arise during mergers, such as tidal debris.

Much work has been done to understand the physical processes driving galaxy evolution in the merger of massive galaxies. It has been shown by many observational and theoretical studies that, during the intermediate phases of interactions, large scale tidal interactions trigger the formation of peculiar features like shells, streams, bridges and tails (Toomre & Toomre 1972; Eneev et al. 1973; Barnes & Hibbard 2009; Struck & Smith 2012; Duc & Renaud 2013). The presence of such structures, which is also predicted by numerical simulations, is now frequently observed in deep imaging surveys (Conselice & Gallagher 1999; Smith et al. 2007; Tal et al. 2009; Duc et al. 2011, 2014b; Kim et al. 2012; Struck 1999; van Dokkum 2005).

In the low mass regime, a detailed study of interacting systems has been exceptionally rare. This is likely because such systems are not as easy to observe as in massive systems. A part of the reason for this could perhaps be that the tidal features which are produced are not as spectacular as in merging giant galaxies due to the relatively weak tidal forces acting upon them. But certainly dwarf galaxies, by nature, are inherently low surface brightness systems and thus the tidal feature emerging from them are often even more low-surface brightness, making them challenging to detect. Only recently, with the advent of low surface brightness imaging techniques, and dedicated data reduction procedures, have we been able to better detect such features (Abraham & van Dokkum 2014; Duc et al. 2014a; Mihos et al. 2017).

Dwarf-dwarf interactions might also be distinct from giant-giant interactions for another reason. In low density environments, dwarfs are often much more gas rich than giant galaxies. Furthermore, the dynamics of gas is not scalable in the same way that the dissipationless star and dark matter components are. For example, the neutral hydrogen in galaxies has a typical velocity dispersion of ~ 10 km/s. For giants, with rotation velocities

of more than 100 km/s, this internal velocity may have a minor contribution to the overall disk dynamics. However for dwarf galaxies, a 10 km/s velocity dispersion can make a significant contribution to the internal dynamics. This may potentially lead to a difference in the star-formation efficiency and overall evolutionary history of dwarf galaxies compared to giants.

A few detailed observational studies of some individual dwarf galaxies with merging feature have been reported in recent years (Rich et al. 2012; Paudel et al. 2015; Pearson et al. 2016; Annibali et al. 2016). In our nearby vicinity, apart from the infamous interaction between the Magellanic clouds, there is also NGC 4449, an ongoing interaction between a Magellanic type dwarf and its nearby dwarf companions (Putman et al. 2003; Martínez-Delgado et al. 2012; Rich et al. 2012; Besla et al. 2016) in which a small stretched stellar stream is observed at the edge of the NGC 4449. The presence of a shell feature in the Fornax dwarf spheroidal has also been interpreted as a relic of a recent merger (Coleman et al. 2004; Yozin & Bekki 2012). In addition to this, Paudel et al. (2015) reported interactions between dwarf galaxies where the overall morphological appearance is similar to that of the well known giant system Arp 104. Also there is UM 448, a merging blue compact dwarf galaxy (BCD), which possesses a pronounced tidal tail that was studied in James et al. (2013).

Despite these detailed studies of a few intriguing examples, very little is known about whether these systems are representative of dwarf-dwarf interactions in general. Nevertheless, given that the majority of galaxies in the Universe are dwarfs, it is clearly important to know how dwarf galaxies evolve through the merging process. Dwarf galaxies not only differ in mass from giant galaxies, but they also have higher gas mass fractions and lower star-formation efficiencies. Low mass galaxies are also typically dominated by exponential disks. How might these properties affect the interaction compared to their giant counterparts? Despite the very similar visual morphology of UGC 6741 system to Arp 104, Paudel et al. (2015) reported a number of star forming region in the bridge connecting the two interacting galaxies, whereas such star formation is completely absent in Arp104 (Gallagher & Parker 2010). Dwarf galaxies, by definition can exert lower tidal forces compared to their massive counterparts – does this result in differences in the tidal features compared to those produced by the much stronger tidal forces of giant galaxies? Antenne (NGC 4038/39), Mice (NGC 4676), Tadpole (UGC 10214) and Guitar (NGC 5291) are some spectacular examples of tidal features that we observe in the interactions between giant galaxies. In addition to this, prominent shell features (e.g. NGC 747 or NGC 7600) are also commonly observed in giant elliptical galaxies (Duc et al. 2015).

Recently, a systematic study of dwarf galaxy pairs, likely to be interacting, in the SDSS data base has been

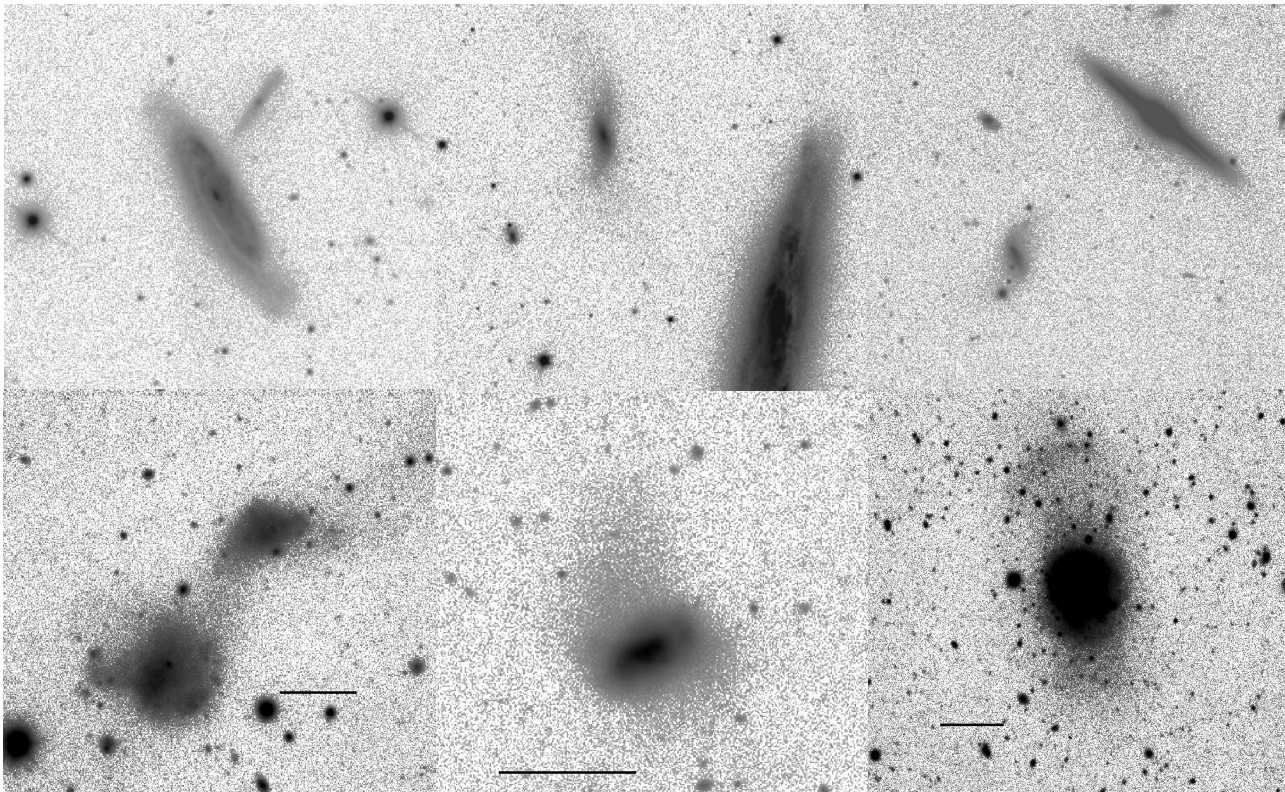


Figure 1. Representative examples of dwarf galaxies with tidal features.

Top: Examples where we conclude a dwarf galaxy is interacting with, and being deformed by the tidal field of a nearby giant galaxy and they have been excluded from the catalog.

Bottom: Examples of dwarfs that we classify as having interacted with another dwarf, categorized into three different types of tidal features (i.e. from left to right; interacting, tidal tail and shell features). For all images, the black horizontal bar represents a scale of $30''$.

presented by Stierwalt et al. (2015), although the full catalog of 104 dwarf-dwarf pair galaxies with the name and position of the galaxies has yet to be publicly released. They are mostly gas-rich and star forming systems, located in low density environments. A sub-set of this sample is studied in Pearson et al. (2016), where their HI morphology is analyzed. They find an extended HI morphology in their tidally interacting galaxy sample compared to non-paired analogues. In this work, we focus on the optical morphology of dwarf-dwarf galaxy interactions. For this, we first create a sample of interacting dwarf galaxies based on a visual analysis of color images from the Sloan Digital Sky Survey (SDSS). We have conducted a systematic search for dwarf galaxies possessing tidal feature, such as stellar streams, shells or filaments, through a careful examination of the SDSS images. Although these features could also be produced by interactions with other galaxies, in this work we try to focus on a sample of dwarf galaxies with tidal features that are likely produced by dwarf-dwarf mergers.

Without aiming to provide detailed science of dwarf-dwarf mergers in this study, we instead aim to provide a sample of dwarf-dwarf merging systems that can later be used for more detailed science. Given the fairly good

number statistics of our sample, we also attempt to understand their typical environment.

For this work, we adopt a standard cosmological model with the following parameters: $H_0 = 71 \text{ km s}^{-1} \text{ Mpc}^{-1}$, $\Omega_m = 0.3$ and $\Omega_\Lambda = 0.7$.

2. SAMPLE SELECTION

2.1. Selection of dwarf-dwarf interactions

Our main aim is to create a large catalog of merging dwarf galaxies. We are mostly interested in dwarf galaxies with tidal features that are likely to be produced by interacting/merging dwarf galaxies. We first search for such disrupted candidates in the large imaging database of the SDSS and the Legacy survey¹.

For this, we use a visual inspection of the true color images from the SDSS-III (Aihara et al. 2011) and the Legacy survey (Blum et al. 2016). The parent sample of galaxies is drawn using a query in the NED where we select galaxies within a redshift range of $z < 0.02$ from the region of sky covered by the SDSS and Legacy survey. We start by selecting galaxies of magnitude $M_r > -19$

¹ <http://legacysurvey.org>

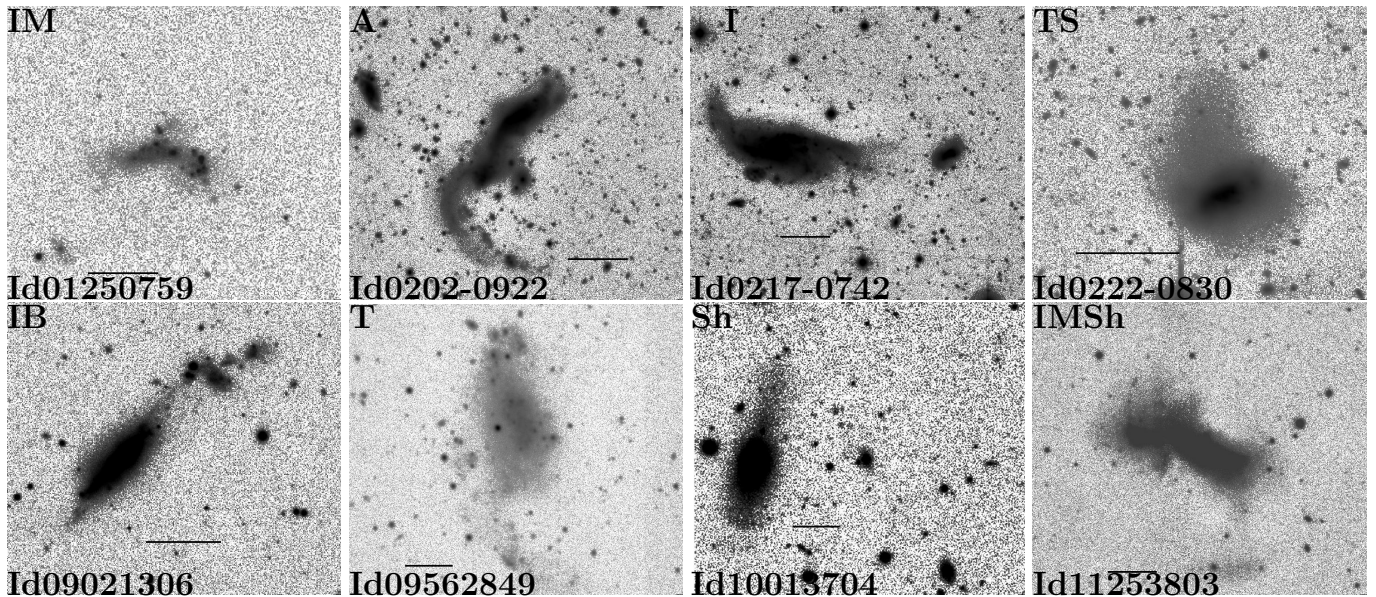


Figure 2. Representative examples of the different morphological classes by which we categorize our merging dwarf galaxies. The field of view and color stretching is arbitrarily chosen to make best view of both interacting galaxies and low-surface brightness features. An image scale of $30''$ is shown by the black horizontal bar. See §2.2 for further details. The complete list of images is shown in Figure 12.

mag to ensure the parent sample of galaxies is predominantly composed of dwarf galaxies. However, note that this magnitude cutoff is only to select the parent sample and we apply a further stellar mass constrain to select the final sample. The stellar mass of candidate galaxies in this sample are measured from our own photometric measurement as described in §3. The total number of galaxies in this redshift range is $\approx 20,000$.

We then extract a cut-out color image from the SDSS sky-server and Legacy survey. As our prime goal is to find tidal debris around the dwarf galaxies, we first collect a sample of dwarf galaxies with observed tidal debris, without considering the origin of the debris at this stage. As might be expected, the majority of the tidal feature are created by interactions with their neighbor giant galaxies. This large sample of disrupted galaxies or galaxies that exhibit tidal debris contain more than 700 candidates. However, for this particular work, we focus on dwarf-dwarf interactions. Another comprehensive catalog of tidally interacting dwarf galaxies with nearby giant galaxies, similar to those studied in Paudel et al. (2014), will be published later (Paudel et al in preparation).

Our visual inspection process involves multiple steps. First, we look for any signature of tidal features in the true color images. If a hint is found, we then re-examine the coadded fits file of the multiple bands available in the archive. The coaddition provides higher SNR than the single band images. Additionally, we also search for the availability of deeper images in various publicly available archives. In this regard, the archival images

of the CHFT² were very helpful for visual confirmation of the presence of low surface brightness feature around dwarf galaxies. From the CHFT archive, we use the Megapipe stack³ produced by The Elixir System (Gwyn 2008). Megapipe stack images are a pipeline reduced images of CHFT MegaCam observation.

Finally, we classify the dwarf galaxies with tidal feature into two broad categories; dwarf-dwarf interaction/merger and dwarf-giant interactions. We show examples of these two classes in Figure 1. The first row shows images of the tidal distortion of dwarf galaxies by nearby giant galaxies and in the second row we show examples of merging dwarf galaxies. It is not always trivial to determine if the observed tidal features were created by merging dwarf galaxies except when the interacting pair have not completely merged yet – like, for example, in the Antennae-like dwarf galaxies (see lower left panel of Figure 1) or simply interacting pairs (see lower middle panel of Figure 1). However, from our past experience, we can often suspect a particular origin according to the appearance of the observed low-surface brightness tidal features. For example, we have shown that shell features about dwarf galaxies are well produced by a merger origin (Paudel et al. 2017). Meanwhile, an S-shaped elongated stellar envelope is likely to be produced by tidal stretching from a nearby giant galaxy (Paudel et al. 2013; Paudel & Ree 2014). These selection criteria are indeed subjective. But, we are keen to

² <http://www.cfht.hawaii.edu/>

³ <http://www.cadc-ccda.hia-ihp.nrc-cnrc.gc.ca/en/megapipe/>

avoid including dwarfs that are interacting with a giant galaxy in this catalog. This may create a bias against merged dwarfs near giants, see discussion §6.

2.2. Sample classification

The final sample consists of 177 systems with a limit in the combined stellar mass of the system of $<10^{10} M_{\odot}$.

We further classify these objects according to the morphology of their tidal features, mainly grouping them into three categories; Interacting, Shell and Tidal tail features. In addition to this, in some cases, we further sub-classify them according to the details of observed low surface brightness feature, see below.

Table 1. Physical properties merging dwarf galaxies.

No.	ID	RA	Dec	z	m_g	m_r	m_{FUV}	m_{NUV}	Feature	Galaxy
		deg	deg		mag	mag	mag	mag		name
001	Id01130052	018.4138	00.8741	0.0039	15.87	15.76	16.79	16.96	I	UGC 00772
002	Id01250759	021.3957	07.9908	0.0097	15.18	15.14	15.89	15.89	IM	UGC 00993
003	Id01482838	027.1545	28.6427	0.0125	15.78	15.35	17.28	16.64	IB	
004	Id0155-0011	028.9989	-0.1855	0.0121	16.47	16.01	17.76	16.55	Sh	
005	Id0202-0922	030.6615	-9.3703	0.0180	15.43	15.13	17.38	17.18	A	PGC007782
006	Id02032202	030.8279	22.0441	0.0088	13.86	13.55	14.15	14.64	IM	UGC 01547
007	Id0210-0124	032.5408	-1.4013	0.0119	15.03	14.83	15.63	16.18	E	KUG 0207-016A
008	Id0217-0742	034.3948	-7.7040	0.0160	14.76	14.45	15.68	16.18	I	PGC008757
009	Id0221-0928	035.4799	-9.4766	0.0123	16.01	15.81	17.20	16.64	I	
010	Id0222-0830	035.5498	-8.5101	0.0156	15.25	14.90	17.15	17.04	TS	
011	Id0227-0837	036.9460	-8.6261	0.0167	16.41	16.09	17.03	17.70	TS	
012	Id02430338	40.82292	3.64472	0.0140	15.08	14.94	I	PGC010297
013	Id07183123	109.6395	31.3866	0.0114	14.41	14.02	I	
014	Id07551505	118.8437	15.0938	0.0154	14.77	14.50	16.37	15.71	IM	PGC022184
015	Id08012517	120.3283	25.2899	0.0155	15.40	15.18	I	PGC022495
016	Id08092137	122.4474	21.6215	0.0111	15.98	15.75	16.42	15.34	T	
017	Id08114627	122.7846	46.4656	0.0074	13.87	13.69	...	14.63	I	PGC022955
018	Id08213419	125.4696	34.3272	0.0077	16.49	16.31	I	
019	Id08291427	127.3861	14.4518	0.0197	16.02	15.72	16.86	16.42	I	
020	Id08331920	128.3229	19.3466	0.0193	14.97	14.68	16.54	16.00	IM	
021	Id08332932	128.3457	29.5386	0.0069	13.06	12.73	14.64	14.35	I	
022	Id08350340	128.8927	03.6717	0.0131	16.96	16.71	T	
023	Id08360509	129.1278	05.1659	0.0135	15.56	15.40	16.68	15.94	I	
024	Id0851-0221	132.9080	-2.3660	0.0109	13.62	13.38	14.86	15.28	I	UGC 04638
025	Id08580619	134.6239	06.3213	0.0119	15.51	15.14	16.70	16.23	IB	UGC 04703
026	Id09003543	135.0654	35.7276	0.0101	13.47	13.26	15.04	14.71	I	NGC 2719
027	Id09002536	135.0999	25.6147	0.0060	14.24	14.14	15.82	15.49	T	
028	Id09021306	135.6726	13.1077	0.0164	14.78	14.48	16.55	16.00	IB	PGC025403
029	Id09114239	137.7848	42.6562	0.0060	15.56	15.31	16.39	15.37	I	
030	Id09164259	139.1047	42.9916	0.0085	14.77	14.57	I	PGC026162

Table 1 continued

Table 1 (continued)

No.	ID	RA	Dec	z	m_g	m_r	m_{FUV}	m_{NUV}	Feature	Galaxy
		deg	deg		mag	mag	mag	mag		name
031	Id09165946	139.1834	59.7746	0.0137	14.88	14.60	16.10	15.93	I	MRK 0019
032	Id09201920	140.1685	19.3374	0.0139	15.96	15.70	17.09	16.58	I	
033	Id09296627	142.2739	66.4579	0.0115	14.97	14.75	16.37	16.03	I	UGC 05042
034	Id09306026	142.5268	60.4481	0.0136	15.21	15.07	16.02	15.74	I	
035	Id09333336	143.4291	33.6002	0.0052	15.32	14.98	16.77	16.83	Sh	KUG 0930+338
036	Id09381942	144.5608	19.7111	0.0144	17.19	16.99	Sh	
037	Id09420929	145.7212	9.49164	0.0107	14.26	14.13	15.31	15.07	I	UGC 05189
038	Id0944-0039	146.0300	-0.6598	0.0041	14.85	14.65	16.09	15.62	I	UGC 05205
039	Id09494402	147.2779	44.0477	0.0156	15.88	15.76	16.68	15.97	I	
040	Id09514419	147.9137	44.3190	0.0150	16.18	15.99	17.03	16.79	I	
041	Id09516853	147.9874	68.8841	0.0146	16.93	16.49	19.10	19.40	I	
042	Id09530702	148.4811	07.0465	0.0174	16.23	15.98	17.79	17.85	L	
043	Id09550823	148.8737	8.39062	0.0041	14.77	14.38	16.33	15.49	Sh	UGCA 188
044	Id09562849	149.1918	28.8288	0.0015	14.38	14.33	15.56	15.49	T	
045	Id10004531	150.0195	45.5198	0.0056	16.50	16.35	I	KUG 0956+457
046	Id10004311	150.0242	43.1919	0.0056	15.31	15.02	Sh	
047	Id10013704	150.3099	37.0709	0.0048	15.33	15.19	16.71	16.10	Sh	PGC029004
048	Id1007-0631	151.8945	-6.5232	0.0158	15.31	14.99	16.30	16.76	IM	
049	Id10080227	152.0430	02.4634	0.0068	14.96	14.24	17.93	16.82	E	PGC029471
050	Id10100509	152.6575	05.1502	0.0137	14.85	14.48	16.38	17.18	S	CGCG 036-048
051	Id10170419	154.2989	04.3312	0.0045	15.63	15.35	17.40	17.22	IB	UGC 05551
052	Id10174308	154.3874	43.1448	0.0037	16.14	15.80	Sh	KUG 1014+433
053	Id10192117	154.7562	21.2836	0.0036	14.56	14.34	16.21	15.94	TS	PGC030133
054	Id10251708	156.2691	17.1494	0.0025	11.54	11.30	12.29	12.87	TS	NGC3239
055	Id10291610	157.4553	16.1809	0.0108	15.12	14.89	16.96	17.18	SL	MRK 0631
056	Id1034-0221	158.5039	-2.3663	0.0067	15.15	15.13	15.63	15.95	T	PGC031246
057	Id10345046	158.6911	50.7683	0.0020	14.14	13.78	15.53	...	I	UGC 05740
058	Id10354614	158.8002	46.2367	0.0016	16.68	16.41	18.44	17.51	Sh	
059	Id10531646	163.3549	16.7711	0.0035	12.58	12.33	13.69	14.18	I	PGC032694
060	Id10535707	163.4561	57.1186	0.0064	13.75	13.45	15.46	14.77	T	NGC 3440
061	Id10545418	163.6635	54.3052	0.0045	11.99	11.63	13.94	13.30	I	NGC3448
062	Id11011636	165.4623	16.6069	0.0098	14.27	13.94	16.26	15.72	F	UGC 06104
063	Id1109-0258	167.4654	-2.9778	0.0172	15.19	14.89	17.05	17.64	I	CGCG 011-014
064	Id11132131	168.4562	21.5205	0.0048	14.66	14.26	I	UGC 06258
065	Id11200231	170.0612	2.52246	0.0054	13.48	13.21	14.98	14.42	I	
066	Id11221319	170.6666	13.3305	0.0137	15.13	14.88	16.27	15.59	I	IC 2776
067	Id11253803	171.3825	38.0605	0.0070	14.24	14.01	15.79	15.70	IMSh	UGC 06433

Table 1 continued

Table 1 (*continued*)

No.	ID	RA	Dec	z	m_g	m_r	m_{FUV}	m_{NUV}	Feature	Galaxy
		deg	deg		mag	mag	mag	mag		name
068	Id1125-0039	171.4670	-0.6615	0.0187	16.44	16.17	17.76	17.20	I	SHOC 324
069	Id11292034	172.3137	20.5831	0.0047	14.02	13.72	15.70	15.53	IMSh	IC 0700
070	Id11350233	173.7706	02.5513	0.0174	15.05	14.81	16.70	16.46	T	UGC 06558
071	Id11351601	173.9550	16.0266	0.0172	16.89	16.62	IB	
072	Id11401924	175.1175	19.4097	0.0113	15.26	14.84	Sh	KUG 1137+196
073	Id11414623	175.3414	46.3932	0.0024	15.09	14.74	17.30	16.63	E	PGC036272
074	Id11412457	175.3545	24.9516	0.0113	15.26	14.83	16.84	17.66	TE	KUG 1138+252
075	Id11451711	176.4793	17.1923	0.0110	15.82	15.71	17.54	17.41	I	UGC 06741
076	Id1148-0138	177.0757	-1.6399	0.0130	15.88	15.66	16.94	16.92	Sh	UM 454
077	Id11501501	177.5113	15.0231	0.0024	14.81	14.72	Sh	MRK 0750
078	Id11502557	177.5840	25.9618	0.0125	13.90	13.57	15.89	15.40	I	UGC 06806
079	Id1152-0228	178.1549	-2.4694	0.0034	14.18	14.10	15.13	...	E	UGC 06850
080	Id11563207	179.1355	32.1303	0.0102	15.89	15.82	16.79	16.51	I	
081	Id12002453	180.0115	24.8892	0.0112	16.86	16.53	18.22	17.29	E	
082	Id12032526	180.9725	25.4352	0.0107	14.00	13.72	14.82	15.25	IM	UGC 07040
083	Id12065858	181.5600	58.9711	0.0108	15.36	15.26	16.47	16.11	I	PGC038384
084	Id12111929	182.9358	19.4906	0.0116	15.03	14.62	T	PGC038842
085	Id12131705	183.2770	17.0988	0.0143	15.53	15.20	17.18	16.63	TS	MRK 0762
086	Id12242109	186.0920	21.1569	0.0031	14.81	14.36	16.69	17.49	Sh	UGC 07485
087	Id12241323	186.1191	13.3858	0.0199	16.47	16.28	17.64	16.87	I	VIII Zw 186
088	Id12250548	186.4687	05.8095	0.0050	14.83	14.54	16.63	16.18	Sh	VCC0848
089	Id12284405	187.0463	44.0935	0.0006	9.24	9.55	10.86	10.81	I	NGC4449
090	Id12304138	187.6515	41.6436	0.0018	9.68	9.35	12.00	11.44	I	NGC4490
091	Id12324937	188.0033	49.6303	0.0145	15.11	14.89	16.65	16.25	IM	PGC041500
092	Id12383805	189.7371	38.0902	0.0074	15.24	15.00	16.42	16.07	I	UGC 07816
093	Id1239-0348	189.8345	-3.8083	0.0084	15.12	14.90	16.46	15.93	IB	PGC042338
094	Id12394526	189.9053	45.4392	0.0125	15.85	15.48	16.94	16.52	I	
095	Id1241-0007	190.4004	-0.1216	0.0158	15.45	15.07	16.40	17.25	T	UM 512
096	Id12444500	191.0289	45.0050	0.0123	14.37	14.19	15.78	15.45	IB	PGC042874
097	Id12464814	191.5972	48.2352	0.0030	15.17	14.94	16.43	16.20	Sh	UGCA 297
098	Id12474709	191.8241	47.1616	0.0196	15.58	15.07	18.04	17.19	TE	MRK 0225
099	Id1249-0434	192.4243	-4.5797	0.0047	13.84	13.64	14.77	15.10	E	NGC 4678
100	Id12530427	193.3083	04.4650	0.0024	12.92	12.62	14.19	14.61	Sh	NGC 4765
101	Id12540239	193.7166	02.6527	0.0031	13.30	13.11	14.14	14.38	I	NGC 4809/ARP 2
102	Id12561630	194.2144	16.5067	0.0041	15.72	15.09	TE	
103	Id1258-0423	194.6983	-4.3861	0.0047	16.36	16.00	16.86	17.54	T	
104	Id13161232	199.2180	12.5482	0.0032	13.85	13.55	15.43	15.07	Sh	NGC 5058

Table 1 *continued*

Table 1 (*continued*)

No.	ID	RA	Dec	z	m_g	m_r	m_{FUV}	m_{NUV}	Feature	Galaxy
		deg	deg		mag	mag	mag	mag		name
105	Id13193015	199.9133	30.2566	0.0071	13.41	13.03	15.92	15.38	T	NGC 5089
106	Id1328-0202	202.1943	-2.0380	0.0123	14.29	13.91	15.45	15.87	TS	PGC047278
107	Id13303119	202.5723	31.3327	0.0161	14.46	14.29	15.82	15.47	IM	UGC 08496
108	Id13335449	203.2852	54.8275	0.0176	15.49	15.19	E	PGC047713
109	Id13343125	203.5622	31.4250	0.0166	14.97	14.77	16.27	15.89	I	UGC 08548
110	Id13425241	205.7475	52.6883	0.0059	16.18	15.87	I	MRK 1481
111	Id13433644	205.8047	36.7493	0.0197	15.64	15.28	16.75	15.84	TS	
112	Id13434311	205.8624	43.1885	0.0083	16.18	15.98	17.82	17.17	Sh	
113	Id13493743	207.4594	37.7306	0.0081	16.01	15.70	17.09	17.36	IB	
114	Id13516422	207.9732	64.3728	0.0058	15.11	14.93	16.27	15.88	IM	PGC049221
115	Id1355-0600	208.9394	-6.0028	0.0066	14.48	14.21	15.25	15.68	I	PGC049521
116	Id1356-0441	209.1966	-4.6923	0.0098	16.99	16.81	17.00	17.78	T	
117	Id13563656	209.2236	36.9454	0.0197	17.59	17.45	17.07	16.06	I	
118	Id14005514	210.1351	55.2460	0.0127	16.04	15.91	16.83	16.59	I	
119	Id14010759	210.4178	07.9979	0.0179	16.93	16.59	18.53	17.48	I	
120	Id14041243	211.2216	12.7288	0.0136	13.81	13.60	14.20	14.35	I	UGC 09002
121	Id1410-0234	212.5531	-2.5744	0.0051	13.44	13.15	15.34	15.18	IM	UGC 09057
122	Id14182530	214.6066	25.5018	0.0149	15.25	14.92	LS	PGC051103
123	Id14182149	214.6805	21.8175	0.0085	14.66	14.71	15.79	15.53	IM	PGC051120
124	Id1421-0345	215.3427	-3.7588	0.0091	14.44	14.24	...	15.59	LS	PGC051291
125	Id14294426	217.4622	44.4476	0.0092	14.46	14.24	16.37	16.00	IM	PGC051798
126	Id14312714	217.7876	27.2373	0.0150	14.41	14.26	I	MRK 0685
127	Id14362827	219.0358	28.4505	0.0063	15.43	15.14	16.75	16.43	Sh	HARO 43
128	Id14365127	219.1908	51.4597	0.0078	15.56	15.13	17.38	16.87	E	PGC052226
129	Id14392323	219.9387	23.3965	0.0150	15.73	15.60	17.38	16.74	I	UGC 09450
130	Id14453124	221.3852	31.4155	0.0049	14.65	14.56	15.38	14.97	I	UGC 09506
131	Id1448-0342	222.2000	-3.7163	0.0031	14.24	13.98	14.96	15.26	I	PGC052893
132	Id14493623	222.4531	36.3965	0.0062	16.33	16.22	17.16	16.90	I	
133	Id14503534	222.7356	35.5721	0.0039	14.41	14.29	15.12	15.00	I	UGC 09560
134	Id14543012	223.5488	30.2095	0.0094	14.72	14.60	15.87	15.65	A	UGC 09588
135	Id14572640	224.4108	26.6683	0.0042	15.41	15.15	16.88	17.21	S	
136	Id15052341	226.3632	23.6883	0.0162	15.35	15.09	17.45	16.81	A	UGC 09698
137	Id1507-0239	226.7837	-2.6627	0.0068	16.21	15.96	17.33	17.27	I	
138	Id15075511	226.9514	55.1857	0.0111	13.99	13.63	21.70	19.67	Sh	UGC 09737
139	Id15091950	227.3164	19.8486	0.0158	16.99	16.58	18.42	17.69	I	
140	Id15174257	229.3553	42.9559	0.0178	15.60	15.23	17.15	16.65	IM	PGC054571
141	Id15182205	229.6666	22.0863	0.0158	15.50	15.11	17.09	17.47	T	PGC054647

Table 1 *continued*

Table 1 (*continued*)

No.	ID	RA	Dec	z	m_g	m_r	m_{FUV}	m_{NUV}	Feature	Galaxy
		deg	deg		mag	mag	mag	mag		name
142	Id15271117	231.8578	11.2842	0.0129	16.14	15.75	TS	
143	Id15271258	231.9358	12.9708	0.0128	18.63	18.40	17.74	18.54	I	
144	Id15292600	232.3709	26.0075	0.0067	14.97	14.86	I	
145	Id15354648	233.7504	46.8146	0.0188	15.58	15.39	...	16.54	T	I Zw 116
146	Id15353840	233.9737	38.6777	0.0186	14.14	13.95	15.96	15.53	I	
147	Id15363040	234.0806	30.6811	0.0058	14.84	14.59	I	PGC055576
148	Id15480414	237.0172	04.2423	0.0131	16.73	16.47	T	
149	Id15511001	237.7562	10.0311	0.0146	15.88	15.62	16.28	17.02	T	CGCG 078-083
150	Id15541637	238.6718	16.6173	0.0079	14.57	14.14	I	UGC 10086
151	Id16055045	241.4178	50.7544	0.0128	15.66	15.51	16.97	16.49	I	
152	Id16054119	241.4459	41.3182	0.0066	13.14	12.94	14.60	14.29	I	UGC 10200
153	Id16060634	241.6708	06.5808	0.0058	14.69	14.33	16.10	15.57	Sh	PGC057169
154	Id16212838	245.3675	28.6399	0.0029	14.40	14.05	16.01	16.31	Sh	UGC 10351
155	Id16274825	246.9728	48.4248	0.0134	16.47	16.19	17.95	17.29	Sh	
156	Id16312024	247.9531	20.4107	0.0171	14.54	14.36	15.97	15.44	Sh	MRK 0884
157	Id14503534	249.5121	26.4527	0.0144	15.41	15.36	16.44	16.07	E	
158	Id16472105	251.7956	21.0952	0.0090	15.42	15.35	IM	
159	Id17135919	258.2862	59.3277	0.0036	13.98	13.76	15.00	14.72	IM	UGC10770
160	Id2119-0733	319.9287	-7.5523	0.0090	14.11	13.86	15.87	15.59	I	PGC066559
161	Id21421518	325.6345	15.3000	0.0122	15.38	15.15	15.85	16.28	T	AGC 748645
162	Id22021945	330.6332	19.7501	0.0054	13.54	13.21	15.28	14.81	IM	IC 1420
163	Id22080441	332.0383	4.69000	0.0135	14.18	13.98	15.94	15.26	I	PGC068112
164	Id22162255	334.0320	22.9333	0.0128	14.76	14.46	15.79	16.32	Sh	KUG 2213+226
165	Id22271205	336.8610	12.0944	0.0118	15.98	15.65	17.30	17.65	Sh	
166	Id22391352	339.8411	13.8822	0.0173	15.08	14.81	16.77	16.22	Sh	
167	Id23021636	345.7469	16.6052	0.0069	13.47	13.18	T	NGC 7468
168	Id2319-0059	349.9917	-0.9855	0.0121	16.12	15.81	18.01	17.91	TS	
169	Id2320-0052	350.1466	-0.8809	0.0145	16.41	16.20	I	UM 158
170	Id2324-0006	351.0990	-0.1075	0.0090	14.22	14.05	15.49	15.30	I	UGC 12578
171	Id23260157	351.6245	01.9602	0.0172	15.37	15.08	16.58	17.27	Sh	CGCG 380-056
172	Id23261144	351.6595	11.7423	0.0125	14.76	14.45	IM	KUG 2324+114
173	Id23302531	352.5412	25.5327	0.0191	14.54	14.27	...	15.38	IM	III Zw 107
174	Id23312856	352.9928	28.9472	0.0182	14.74	14.77	15.79	15.33	IM	MRK 0930
175	Id23371759	354.3894	17.9962	0.0084	13.79	13.43	IM	UGC12710
176	Id2340-0053	355.1846	-0.8874	0.0191	17.41	17.17	18.06	17.19	IM	
177	Id23591448	359.9042	14.8078	0.0058	13.21	12.82	14.53	14.05	Sh	NGC 7800

Table 1 *continued*

Table 1 (*continued*)

No.	ID	RA	Dec	z	m_g	m_r	m_{FUV}	m_{NUV}	Feature	Galaxy
		deg	deg		mag	mag	mag	mag		name

NOTE—The first column is number. We list the Interacting dwarf (Id), coordinates (RA and Dec) and redshift in columns 2, 3, 4, and 5, respectively. The Ids are in ‘hmdm’ format. FUV, NUV, g, and r photometric data is listed in columns 6-9. We present morphological class of merging dwarf systems, obtained according to § 2.2 in column 10. In the last column we provide Name of galaxies that we found in NED.

- Interacting (I): In this class, we identify ongoing interactions between two dwarf galaxies. If the two interacting dwarf galaxies are visibly distinct, we simply designate it with an ‘I’ (e.g. Id0217-0742), and if they are overlapping, or the progenitor galaxies are not distinct, we also give it an ‘M’ (Merged, e.g Id01250759). Additionally, if we see a bridge connecting the interacting galaxies we add ‘B’ (for bridge, e.g. Id01482838). A dwarf analog of the famous Antennae system (NGC 4038/NGC 4039) is represented by ‘A’ (for Antennae e.g. Id0202-0922).
- Shell (Sh): The presence of shell features can be seen e.g. Id0155-0011.
- Tidal tail (T): Simply defined as the presence of amorphous tidal features, mostly tidal streams or plumes, which can not be placed into the above classifications, e.g Id08092137. We notice that the majority of tidal tails are relatively redder than their galaxy’s main body (so likely a distinct stellar population). Thus, they might better be described as stellar streams, in which case we add an ‘S’, e.g. Id0222-0830. Also, if we see a loop of a stellar stream around the galaxies, we identify this with an ‘L’, e.g. Id09530702.

We show various examples of these classification in Figure 2. It is worth noting that the above classification scheme is not mutually exclusive, and in a number of cases there are overlaps. For example, some interacting galaxies also possess multiple tidal features, like shells or stellar stream, even when the two parent dwarf galaxies are not yet fully merged. Id11253803 is the best example of this kind. We show an example of these different morphological classes of merging dwarf galaxies in Figure 2.

3. DATA ANALYSIS

To perform the photometric analysis and measure the total luminosity, we exclusively use the SDSS image data, unless explicitly mentioned otherwise. This is because the SDSS provides the best homogeneous imaging data. We retrieved archival images from the SDSS-III database (Abazajian et al. 2009). Since the

SDSS data archive provides well calibrated and sky-background subtracted images, no further effort has been made in this regard. We derive the g and r -band magnitudes. To do this, we measure the total flux by placing a large aperture which covers both interacting galaxies and the stellar streams around them. While doing so, unrelated background and foreground objects were masked manually. This procedure is quite straightforward if the interacting galaxies are not well separated or already merged. In the case of interacting systems, when the galaxies involved are well separated (class I), the apertures are chosen in two different ways –first a large aperture covering both the interacting galaxies is used to measure the total flux of the system, as done for the other classes. Additionally, we also use smaller apertures to measure the flux of the individual galaxies. However, we emphasize that we only use the aperture photometry of the individual interacting galaxies to calculate their mass ratio. For the rest of the physical parameters we present in this work, values are given for the total system (e.g. magnitudes, $g - r$ colors, stellar masses and star-formation rates).

There are only six candidate galaxies which are located outside of the SDSS covered region of sky. In these cases, we use images from the Legacy survey. We maintain similar procedures for the aperture photometry as were applied with the SDSS images.

For many galaxies (146 out of 177), we found there were GALEX all-sky survey observations available (Martin et al. 2005). Since they are mostly star-forming, almost all are detected in FUV and NUV-band GALEX all-sky survey images. In these cases, we perform aperture photometry on the GALEX image, following the same procedure as we used for the optical images. However, we only calculate the total UV flux of the systems, and not for the individual galaxies, because the GALEX images have a spatial resolution of only 5” and the individual galaxies are not well resolved.

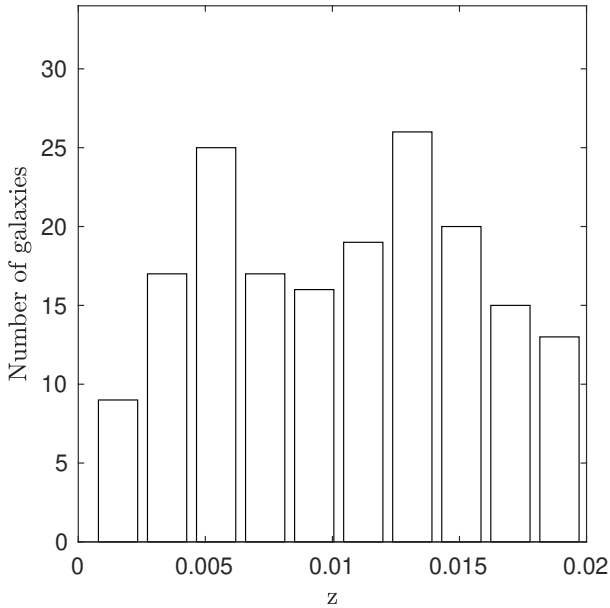
The distances to the galaxies are taken from NED. For those where NED does not provide a redshift independent distance, we calculate it based on Hubble flow assuming the cosmological parameters defined in §1. We use the python code, COSMOCALC, available in ASTROPY to calculate cosmological distances based on the radial velocities. The radial velocities are not corrected for Virgo-centric flow.

Table 2. Derived properties of merging dwarf galaxies

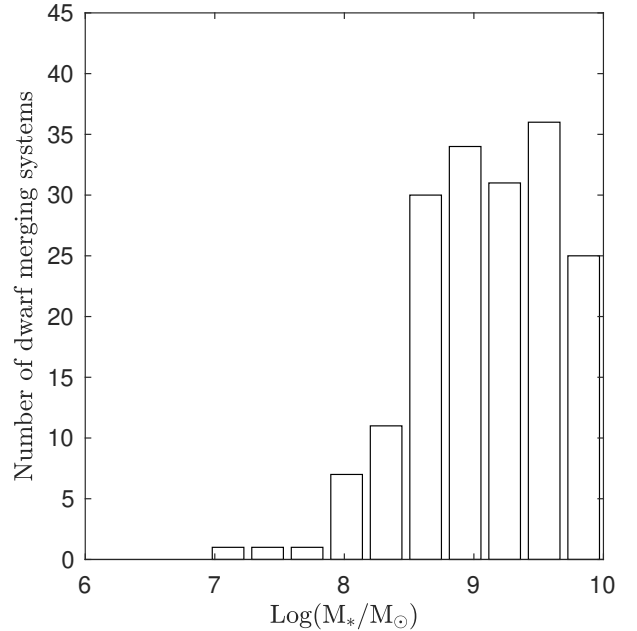
Number	Distance	g-r	M_B	M_*	M1:M2	SFR	M_{HI}	Set	no. neighbor
	Mpc	mag	mag	$\log(M_\odot)$		$\log(M_\odot/\text{yr})$	$\log(M_\odot)$		
(1)	(2)	(3)	(4)	(5)	(6)	(7)	(8)	(9)	(10)
001	16.52	0.11	-14.96	7.81	5	-1.51	8.49	1	22
002	41.26	0.04	-17.66	8.78	2	-0.35	9.30	0	9
003	53.29	0.43	-17.49	9.35	4	-0.68	8.76	1	3
004	51.57	0.46	-16.72	9.09	...	-0.91	8.43	0	3
005	77.06	0.30	-18.68	9.61	...	-0.40	...	0	1
.....

NOTE—A portion of the Table is shown here for guidance regarding its contents and form. The table in its entirety will be published as part of the online catalog.

Col.(1): Number, Col.(2): Adopted distance to the galaxy, Col.(3): g-r color, Col.(4): B-band absolute magnitude, Col.(5): Stellar mass, Col.(6): Mass ratio of interacting galaxies, Col.(7): Star formation rate, Col.(8) HI mass: , Col.(9): Satellite or not – 1 for yes and 0 for no, Col.(10): Number of neighboring galaxies within our search criteria – see text §3.

**Figure 3.** Redshift distribution of the sample

The derived magnitudes were corrected for the Galactic extinction using [Schlafly & Finkbeiner \(2011\)](#), but not for internal extinction. The star formation rates (SFRs) are derived from the FUV fluxes applying a foreground Galactic extinction correction ($A_{FUV} = 7.9 \times E(B-V)$ [Lee et al. 2009](#)). We use the equation ($\text{SFR}(M_\odot \text{ yr}^{-1}) = 1.4 \times 10^{-28} L_\nu(\text{UV})(\text{erg s}^{-1} \text{ Hz}^{-1})$ [Kennicutt 1998](#)). The stellar masses were derived from the SDSS-*r* band magnitude with a mass to light ratio tabulated by [Bell et al. \(2003\)](#) appropriate to the observed $g-r$ color.

**Figure 4.** Distribution of the logarithm of the stellar mass of merging dwarf systems.

4. RESULTS

Our morphological classification reveals that there are 98 interacting dwarf galaxy systems. Among these, 22 are classified ‘Interacting Merger’ (IM) type where the boundary between the interacting galaxies can no longer be clearly identified. 30 possess shell features and the rest (49) show tidal tails of different forms. The shell features are mainly found outside of the main body of the galaxies. Some of these resemble the dwarfs with

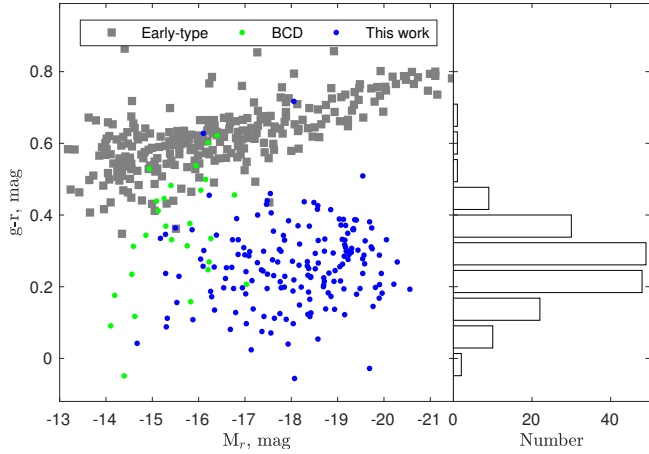


Figure 5. The optical color-magnitude relation. Blue dots represent interacting dwarfs. The comparison sample are early-type galaxies (gray square) and BCDs (green dots) taken from Janz & Lisker (2009) and Meyer et al. (2014), respectively.

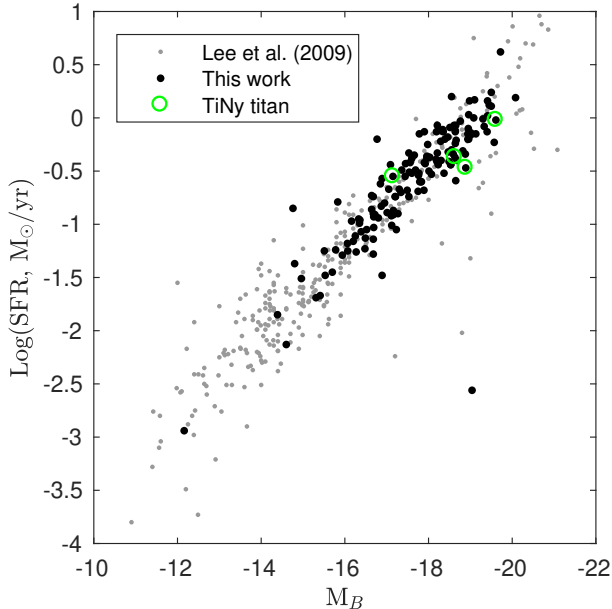


Figure 6. Relation between star-formation rate versus blue-band absolute magnitude. The black symbol represents merging dwarf systems and gray symbols are the Lee et al (2009) galaxies. Those interacting pairs that are found in both our sample and those of the Tiny titan sample are shown with green circles.

the symmetrical-shaped shell features that were found in Paudel et al. (2017) (e.g. Id09381942, Id10354614, Id12464814). In Paudel et al. (2017), we studied three dwarf galaxies and, with help of idealized numerical simulation, found that they had suffered a very recent (in last few hundred Myr), near equal mass merger which explained their symmetry. However, in some cases, the

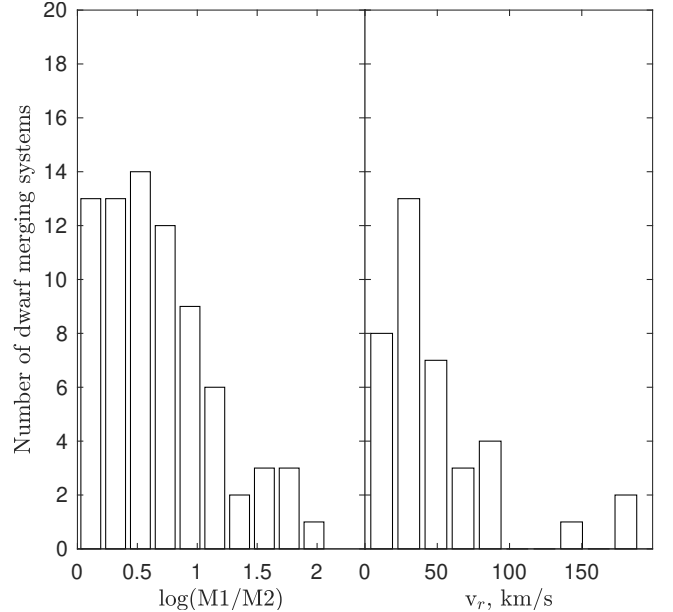


Figure 7. Distribution of mass ratio and relative line of sight velocity of interacting dwarf pairs. Each panel contains different numbers of galaxies; for the mass ratio there are 76 and for the velocity separation there are 38, for the reasons given in the text, see §4

shell dwarfs do not show such symmetry in their shells (e.g. Id11253803) and in two we find that shell and tidal tails features coexist with each other (Id11253803 and Id11292034). In these cases, the shells are generally higher surface brightness than the tidal tails.

There are three dwarf galaxy systems (Id0202-0922, Id1448-0342, Id14503534) which can be considered dwarf analogues to the Antennae system (NGC 4038/4039).

We present the result of aperture photometry in Table 1. We list the positions (RA and DEC) and redshift of candidate dwarf galaxies in column 2, 3 and 4, respectively. Optical g and r band magnitude are listed in column 5 and 6, respectively. Next we list FUV and NUV band magnitudes in the column 7 and 8, respectively. The classification of morphological feature are given in column 9.

We show the redshift distribution of our catalog of dwarf galaxies in Figure 3. The median redshift of this sample is 0.01. Next, we show the total stellar mass distribution of interacting/merging dwarf galaxies in Figure 4. It is not surprising that this sample is somewhat biased towards the brighter end of our stellar mass cut. Nevertheless, the range of stellar mass coverage is of order 3 magnitudes, with the median value of $\log(M_*/M_\odot) = 9.1$. The minimum mass galaxy, Id10354614, has a similar stellar mass to the local group Fornax dwarf galaxy or Virgo cluster dwarf galaxy VCC1407, both are well known for their shell feature and well discussed

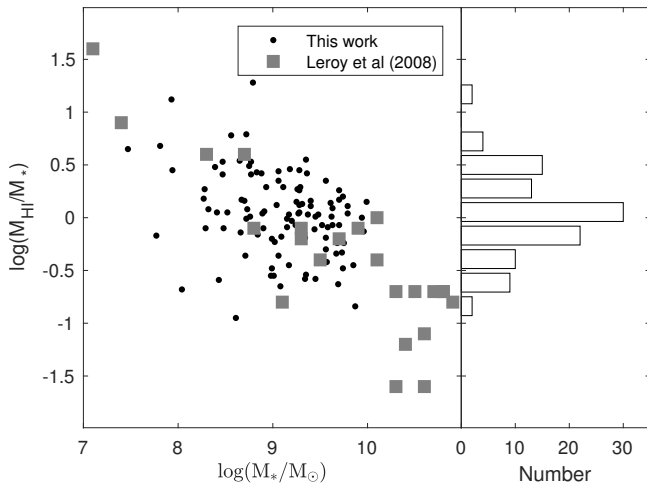


Figure 8. Relation between gas mass fraction and stellar mass. The comparison data is from Leroy et al. (2008).

as a merger remnant (Paudel et al. 2017; Coleman et al. 2004).

The $g - r$ color distribution shown in Figure 5 right panel, reveals that this sample is overwhelmingly dominated by star-forming galaxies with similar colors to Blue Compact Dwarf galaxies (BCDs Meyer et al. 2014). Our sample has a median value of $g - r$ color index = 0.32 mag. For comparison, we also show a sample of early-type galaxies from Janz & Lisker (2009) which clearly offsets from our sample galaxies, creating a red-sequence above the star-forming galaxies in the color-magnitude relation. In fact, there are only three galaxies (Id10080227, Id12474709 and Id12561630) which have a $g - r$ color index more red than 0.5 mag and they are also morphologically akin to the early-type galaxies.

As previously mentioned, the overwhelming majority of galaxies in this sample are blue and they are also detected in the GALEX all sky survey FUV band image which further confirms ongoing active star-formation. Figure 11 illustrates the relation between the B-band absolute magnitude and the star-formation rate. The B-band magnitudes are derived from the SDSS g and r -band magnitudes using the equation $B = g + 0.3130 \times (g - r) + 0.2271$ (Lupton 2005⁴). For comparison, we also plot data from Lee et al. (2009), see gray symbol, who study the FUV-derived star formation rates of local volume (<11 Mpc) star-forming galaxies. From this figure, it is clear that these interacting dwarfs galaxies do not differ from the trend made by local volume star-forming galaxies.

Among the interacting system there are 76 for which we can clearly separate out the individual interacting members (only ‘I’ class), which we will refer to as an ‘interacting dwarf pair’. To measure the mass ratio of

interacting dwarf pair, we perform the aperture photometry in the SDSS r -band images on the individual interacting galaxies. Note that this is actually the flux ratio (larger flux /smaller flux) but, under the assumption of similar stellar populations in both galaxies, we simply use the the term mass ratio. Among the interacting dwarf pairs, we find that both member galaxies share similar $g - r$ colors which also validates our assumption of similar stellar populations. We show the distribution of their mass ratios in Figure 7. It is clear that the majority of interactions are major interaction with a mass ratio of 5 or less, and the median is 4. The first bin of the histogram includes 13 systems (17% of the total) which can be considered equal mass mergers. In reverse, there are 15 systems (20% of the total) which have a mass ratio larger than 10, which can be considered a minor merger. The maximum mass ratio is 120 in the case of Id14392323. Among the 76 dwarf interacting pair we find that there are 38 systems where radial velocities are available for both members of interacting pair dwarf galaxies. As the right panel of Figure 7 indicates, the relative line of sight velocity between the interacting dwarf pairs is relatively low and, only in two cases, it is higher than 100 km/s.

For our sample of merging dwarf galaxies, we also collected neutral Hydrogen (HI) masses from the CDS server⁵. Since this data is assembled from various sources in the literature, we caution about the heterogeneity of the results. The various sources may use different beam sizes, and exposure times, depending on the aim and scope of their individual projects (Paturel et al. 2003; Meyer et al. 2004; Giovanelli et al. 2005; Courtois & Tully 2015). They are mostly from single dish observations, and we expect that a typical beam size of $3'$, like the Arecibo telescope, would be sufficient to entirely cover the interacting dwarf galaxies, and therefore must be considered as measurements for the total, combined system. We found HI masses for 109 merging dwarf galaxies, as listed in Table 2.

Figure 8 reveals the relation between the HI mass fraction and stellar mass of the star-forming galaxies. It is clear from this figure that our interacting dwarf sample clearly follow the HI mass fraction and stellar mass relation of other star-forming galaxies in the local Universe Leroy et al. (2008). We show the distribution of HI mass fraction in the right panel. The median value of the gas mass fraction of our sample is $M_{HI}/M_* = 1.09$.

5. DISCUSSION

In this paper, we present a sample of interacting dwarf galaxy systems. Given the large heterogeneity in the data collection procedure, probably part of the scientific discussion can only be considered as a qualitative. However, merging/interacting dwarf galaxies are not thought

⁴ <http://www.sdss3.org/dr8/algorithms/sdssUBVRITransform.php>

⁵ <http://cdsportal.u-strasbg.fr>

to be a common phenomenon in the local Universe. According to hierarchical cosmology, theory predicts that they are common in the early-universe. To date, no systematic effort has been made to present a sample of interacting dwarf galaxies which is statistical enough to study the properties of interacting dwarf galaxies and their role in the evolution of low mass galaxies. This is the first publicly available catalog in this regard.

5.1. Comparison to previous study

A previous study of interacting pairs of dwarf galaxies, (Stierwalt et al. 2015, here after S15), mainly focuses on a statistical analysis of environmental effects on interacting pairs of dwarf galaxies (Patton et al. 2013). Like in this study, S15 also uses SDSS imaging to select their sample galaxies, therefore we expect that both samples cover the same areas of sky. But probably, the main difference is their redshift coverage. Our sample’s redshift range is <0.02 , while the S15 sample galaxies have redshifts up to 0.07.

In addition to this, S15 performed a careful selection of a control sample and a working sample to remove biases due to the sample selection procedure, when comparing the samples. In contrast, in this work we first aim to present a large catalog of merging dwarf systems which will be helpful for a detailed study of various properties of interacting/merging dwarf galaxies in the future. We provide basic properties, such as sky-position, redshift, stellar-mass and star-formation rate. Further, having these properties in hand we also try to assess the effect of environment on our sample galaxies, comparing gas-mass fraction and star formation rate (SFR) between merging dwarf systems and that of normal galaxies from local volume. We mainly compile our comparison sample data from the literature, thus we caution that our comparative study may not be as statistically rigorous as that of the S15 comparative study between interacting dwarf and non-interacting dwarf galaxies. However, we include the comparison simply to give the properties of our sample some context in comparison to a sample of non-interacting dwarfs of similar mass.

In S15 sample, the pair galaxies needed to have a separation velocity less than 300 km/s which means they required that there be a measured radial velocity for both galaxies. In contrast, we select interacting dwarf galaxies according to their observed tidal features, and it is not necessary to have a radial velocity for both interacting members. This means we are able to study merging dwarfs over a far greater range of merging stages, even when one dwarf has fully merged with another and the only indication of the event might be the remaining tidal features. A good example of this can be found in our shell feature dwarfs.

While comparing S15 sample with only interacting pair (I class), we find significance difference in mass ratio of member dwarf galaxies of interacting pair. S15 overwhelmingly dominated by small mass ratio pairs,

i.e 93% of their sample is less than mass ratio 5 and in our case less than half, only 42% , interacting pair have mass ratio less than 5. In addition, while comparing radial velocity separation between interacting, although we find a relatively low number of systems that have radial velocity measurements for both interacting member dwarf galaxies of our sample, we find a clear difference with S15 – only 2 out of 36 (5%) have a relative line of sight velocity larger than 100 km/s and 15 out of 60 (25%) interacting dwarf pairs in the S15 sample have relative line of sight velocities larger than 100 km/s.

Another interesting difference is that S15 find there is an enhanced SFR between dwarf galaxies at small separations from their partner, compared to a control sample of isolated dwarf galaxies. However, in Figure 6 we find no evidence for an enhanced SFR in our merging dwarf systems compared to a sample of star-forming galaxies of local volume. One reason we see no clear enhancement in SFR could be because we don’t attempt to control for separation distance. Also, S15 compared a homogeneously selected control sample with interacting dwarf-pairs, while we simply use data compiled from the literature as a comparison sample. In fact, a small number of the S15 galaxies can be found in common with this sample, although they follow the same trend as our sample (see Figure 6.)

Another part of the difference could emerge from the way we derived SFR. S15 used catalog values of SFRs from Brinchmann et al. (2004), which is derived from H_{α} emission line flux of the SDSS fiber spectroscopic data. On the other hand, we have used the FUV flux to derive the SFR where the FUV emission traces recent star formation over longer time scales compared to H_{α} . However note that, to derive SFR we have used FUV flux only corrected for foreground Galactic extinction but not internal extinction therefore these values are, in many case, would be a lower limit. In the future, we will consider full SED fitting, including infrared wavelengths, in order to better constrain their SFRs.

5.2. Environment

We now turn to the surrounding environment of our merging dwarf systems. For this work we characterize the surrounding environment by searching for neighboring giant galaxies ($M_K < -20$ mag, corresponding to a stellar mass of $>10^{10}$), within a sky projected distance of less than 700 kpc, and a relative line of sight radial velocity of less than ± 700 km/s. This is the similar criteria that we have previously used to search for isolated early-type dwarf galaxies in Paudel et al. (2014).

We find that only 41 dwarf galaxy merging systems have giant neighbors. The median stellar mass of the giant neighbors is $6 \times 10^{10} M_{\odot}$. For convenience, we called them satellite merging dwarf system and the rests are isolated merging dwarf systems, here after. Among 41 satellite merging systems, there are 19 ‘I’ class systems (interacting dwarf pairs) where we identify ongoing

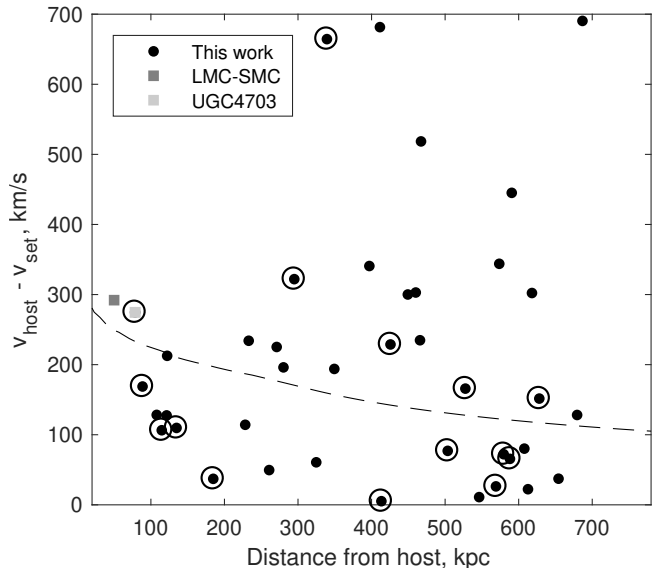


Figure 9. Phase-space diagram of merging satellites. Y-axis is relative line of sight velocity between dwarf-merging system and nearby giant galaxy and X-axis is sky-projected physical distance between them. The dashed line represents the escape velocity as a function of radius for a Milky-Way like galaxy, derived from the best match model in [Klypin et al. \(2002\)](#). We show dwarf interacting pair with a circle. We also show the position of the LMC-SMC pair and UGC 4703 in such a diagram with gray squares.

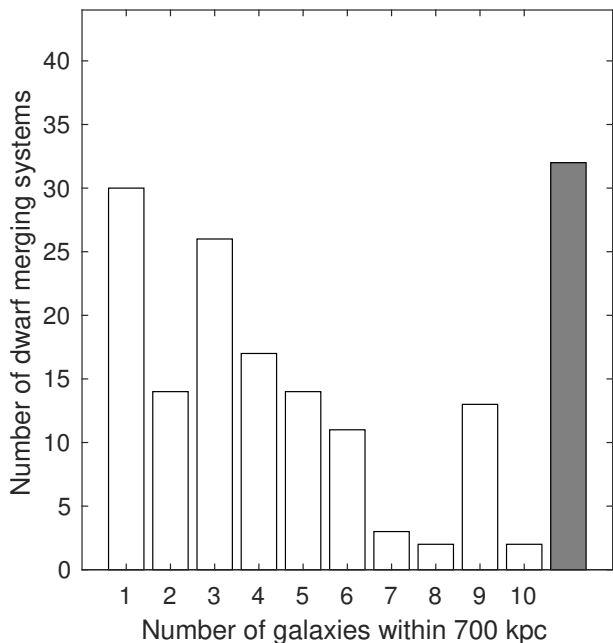


Figure 10. Total number of galaxies, including both giants and dwarfs, within an area coverage of 700 kpc radius and ± 700 km/s line of sight radial velocity around merging dwarf systems. The last gray bar represents number of merging dwarf systems which have more than 10 neighbor galaxies.

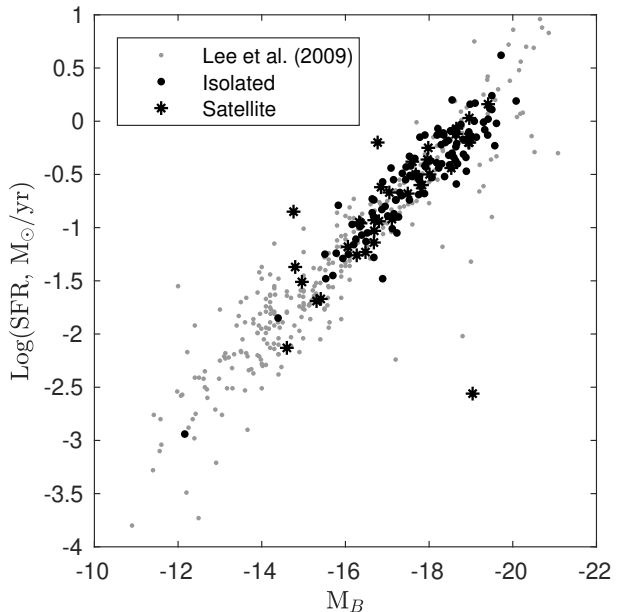


Figure 11. Comparison of the star-formation rates of satellite (star) and isolated (dot) merging dwarfs systems. We also show the local volume (< 11 Mpc) star-forming galaxy sample of [Lee et al. \(2009\)](#) in gray.

interaction between dwarf galaxies. Shell features are found in 10 systems and the remaining 12 are a mixture of E/T/S classes.

Interestingly, all three early-type merging dwarfs are located at large sky projected distance from the giant galaxies, beyond 700 kpc. In fact, [Paudel et al. \(2014\)](#) already pointed out that Id10080227 is a compact elliptical galaxy (cE [Chilingarian \(2009\)](#)), located in isolation, which may have formed through the merging of dwarf galaxies.

In [Figure 9](#), we show a phase space diagram of the satellite merging dwarf systems. It is clear from this figure that our satellite merging dwarf systems are located comparatively farther than the distance of the LMC-SMC system is from the Milky-Way (MW). We also highlight the position of UGC 4703, which we studied as an LMC-SMC-MW analog in [Paudel et al. \(2017\)](#), and lies in a similar region in phase space. The dashed line represents the escape velocity as a function of radius for a Milky-Way like galaxy, based on the best match model to the Milky-way from [Klypin et al. \(2002\)](#). The two highlighted interacting dwarf pairs, LMC-SMC and UGC 4703 are located at small radius and large velocity, near the escape velocity boundary, perhaps indicating they are recent infallers into their host ([Rhee et al. 2017](#)). It seems that only half of the satellite merging dwarf systems are clearly bound to their hosts, (assuming their hosts are MW-like), i.e located below the escape velocity line. The rest are scattered well beyond the escape velocity boundary, and often at distances > 400 kpc which is at least twice the Virial radius of a MW-

like galaxy. Thus it is probable that many of these are not bound to their hosts, and in many cases our selection criteria of 700 kpc search radius and ± 700 km/s velocity range is not robust enough to characterize if our merging dwarfs are hosted by a nearest giant host. The phase space diagram also reveals that there is no special difference between satellite interacting dwarf pairs (shown as empty circle symbols) and the rest of the sample, that have likely already merged (shown as black dot), in their location of their phase-space diagram.

We compare the star-formation rates of candidate satellites and isolated merging dwarf system, see Figure 11. The black dot represent the satellite candidates and blue dots represent isolated. From this figure, it is clear that both the isolated and satellite merging dwarf system have similar star formation properties compared with Lee et al. (2009). We also find only a marginal difference in the distribution of gas mass fraction of satellite and isolated dwarf systems with the median values 1.04 and 1.09, respectively. This is slightly contradictory to the finding of S15, where they found interacting dwarfs located near to the giant galaxy are likely to have a lower gas mass fraction.

We also attempt using number density to characterize the surrounding environment of merging dwarf systems. For this we, simply searched the number of galaxies, both giant and dwarf, within the above mentioned search area (i.e within 700 kpc radius and ± 700 km/s line of sight radial velocity). For this, we also remove those merging dwarf systems which have a line of sight radial velocity less than 900 km/s to avoid distance uncertainties of nearby galaxies.

We find that a significant fraction, 30 out 177, merging dwarf systems have no neighbor, not even another dwarf galaxy, within our search area. In contrast, more than 10 neighbors are found only for 32 cases, and they are mostly interacting satellites. We show a simple histogram of the number of galaxies (which include both giants and dwarfs) found in the search area in Figure 10. The last bin (the gray histogram) represents the number of merging dwarf systems which have more than 10 neighbors within our search area. From this figure, it is clear that the probability of finding a merging dwarf system increases in low density environments. The median neighbor number of merging dwarf systems in this sample is 4.

6. CONCLUSIONS AND REMARKS

We have collected a catalog of 177 merging dwarf systems, spanning the stellar mass range from 10^7 to $10^{10} M_{\odot}$ in a redshift range $z < 0.02$. The sample is overwhelmingly dominated by star-forming galaxies and they are located significantly below the red-sequence in the observed color-magnitude relation. The fraction of early-type dwarf galaxies is only 3 out of 177. Star forming objects may be preferentially selected because of the criterion to have a redshift and it is easy to measure

redshift from emission line of star-forming galaxies than absorption line of non star-forming galaxies.

We classify the morphology of the low surface brightness feature into various categories such as shells, stellar streams, loops, Antennae-like systems, or simply interacting. These different types of low surface brightness features may hint at objects in different stages of their interactions. For example, the shell feature might be the product of a complete coalescence, while two well separated interacting dwarfs are probably in the earlier stages of their interaction. There are three dwarf galaxies (Id0202-0922, Id1448-0342, Id14503534) that can be considered dwarf analogues to the Antennae-system (NGC 4038/4039).

A potential problem with these types of catalog is that they are inherently inhomogeneous and incomplete. Because they are selected from visual inspection of low-surface brightness feature, this depends on the depth of the imaging survey, and on how well defined the tidal features are. As a result, this is in many ways very subjective. We certainly caution on the completeness of the catalog and there maybe many possible biases in our selection procedure. For example, dwarf galaxies with tidal features whose origin is unclear and are located near to a giant ($M_* > 10^{10}$) host galaxy have been selectively removed. That may lead to an artificial reduction in the number of merging dwarf systems near giant galaxies.

However, more isolated dwarf interacting pairs do not suffer this issue, as there is no uncertainty as to whether a giant galaxy is responsible for the observed fine structure (e.g. tidal streams, tails, shells, etc). Therefore, we believe our sample will be more complete for these kinds of objects, as long as the interacting pairs show similar low surface brightness features as presented by our sample. We believe that it makes physical sense that dwarf systems struggle to merge in the presence of a nearby giant galaxy. Dwarf galaxies have small escape velocities, owing to their small masses. As a result only a small amount of peculiar motion, due to the potential well of a giant galaxy, might be enough to make it nearly impossible for dwarfs to meet at low enough velocities to merge. Thus, we suspect that our selection criteria maybe simply enhancing a real dependency on distance to the nearest giant galaxy. In any case, we find that there is no significant difference in the phase-space diagram of dwarf interacting pair (I class) and the rest of the sample.

In conclusion, we present a large set of interacting and merging dwarf systems, including aperture photometry in UV and optical bands, as well as stellar masses, star formation rates, gas masses and stellar mass ratios. This data might be useful for detailed studies of dwarf-dwarf interactions in the near future.

P.S. acknowledges the support by Samsung Science & Technology Foundation under Project Number SSTF-BA1501-0. S.-J.Y. acknowledges support from the Center for Galaxy Evolution Research (No. 2010-0027910) through the NRF of Korea and from the Yonsei University Observatory – KASI Joint Research Program (2018). P.C.-C. was supported by CONICYT (Chile) through Programa Nacional de Becas de Doctorado 2014 folio 21140882.

This study is based on the archival images and spectra from the Sloan Digital Sky Survey and Legacy Survey Data. Their full acknowledgment can be found at <http://www.sdss.org/collaboration/credits.html> and <http://legacysurvey.org/acknowledgment/>, respectively. Funding for the SDSS has been provided by the Alfred P. Sloan Foundation, the Participating Institutions, the National Science Foundation, the U.S. Department of Energy, the National Aeronautics and Space Administration, the Japanese Monbukagakusho, the Max Planck Society, and the Higher Education Funding Council for England. The SDSS Web Site is <http://www.sdss.org/>.

The Legacy Surveys imaging of the DESI footprint is supported by the Director, Office of Science, Office of High Energy Physics of the U.S. Department of Energy under Contract No. DE-AC02-05CH1123, by the National Energy Research Scientific Computing Center, a DOE Office of Science User Facility under the same contract; and by the U.S. National Science Foundation, Division of Astronomical Sciences under Contract No. AST-0950945 to NOAO. We also made use of the GALEX all-sky survey imaging data. The GALEX is operated for NASA by the California Institute of Technology under NASA contract NAS5-98034. We also acknowledge the use of NASA’s Astrophysics Data System Bibliographic Services and the NASA/IPAC Extragalactic Database (NED). We also made use of archival data from Canada-France-Hawaii Telescope (CFHT) which is operated by the National Research Council (NRC) of Canada, the Institut National des Sciences de l’Université of the Centre National de la Recherche Scientifique of France and the University of Hawaii.

REFERENCES

- Abazajian, K. N., Adelman-McCarthy, J. K., Agüeros, M. A., et al. 2009, *ApJS*, 182, 543, doi: [10.1088/0067-0049/182/2/543](https://doi.org/10.1088/0067-0049/182/2/543)
- Abraham, R. G., & van Dokkum, P. G. 2014, *PASP*, 126, 55, doi: [10.1086/674875](https://doi.org/10.1086/674875)
- Aihara, H., Allende Prieto, C., An, D., et al. 2011, *ApJS*, 193, 29, doi: [10.1088/0067-0049/193/2/29](https://doi.org/10.1088/0067-0049/193/2/29)
- Amorisco, N. C., Evans, N. W., & van de Ven, G. 2014, *Nature*, 507, 335, doi: [10.1038/nature12995](https://doi.org/10.1038/nature12995)
- Annibali, F., Nipoti, C., Ciotti, L., et al. 2016, *ApJL*, 826, L27, doi: [10.3847/2041-8205/826/2/L27](https://doi.org/10.3847/2041-8205/826/2/L27)
- Arp, H. 1966, *ApJS*, 14, 1, doi: [10.1086/190147](https://doi.org/10.1086/190147)
- Barnes, J. E., & Hibbard, J. E. 2009, *AJ*, 137, 3071, doi: [10.1088/0004-6256/137/2/3071](https://doi.org/10.1088/0004-6256/137/2/3071)
- Bell, E. F., McIntosh, D. H., Katz, N., & Weinberg, M. D. 2003, *ApJS*, 149, 289, doi: [10.1086/378847](https://doi.org/10.1086/378847)
- Besla, G., Martínez-Delgado, D., van der Marel, R. P., et al. 2016, *ApJ*, 825, 20, doi: [10.3847/0004-637X/825/1/20](https://doi.org/10.3847/0004-637X/825/1/20)
- Blum, R. D., Burleigh, K., Dey, A., et al. 2016, in *American Astronomical Society Meeting Abstracts*, Vol. 228, American Astronomical Society Meeting Abstracts #228, 317.01
- Boselli, A., & Gavazzi, G. 2006, *PASP*, 118, 517, doi: [10.1086/500691](https://doi.org/10.1086/500691)
- Brinchmann, J., Charlot, S., White, S. D. M., et al. 2004, *MNRAS*, 351, 1151, doi: [10.1111/j.1365-2966.2004.07881.x](https://doi.org/10.1111/j.1365-2966.2004.07881.x)
- Chengalur, J. N., Pustilnik, S. A., Makarov, D. I., et al. 2015, *MNRAS*, 448, 1634, doi: [10.1093/mnras/stv086](https://doi.org/10.1093/mnras/stv086)
- Chilingarian, I. V. 2009, *MNRAS*, 394, 1229, doi: [10.1111/j.1365-2966.2009.14450.x](https://doi.org/10.1111/j.1365-2966.2009.14450.x)
- Coleman, M., Da Costa, G. S., Bland-Hawthorn, J., et al. 2004, *AJ*, 127, 832, doi: [10.1086/381298](https://doi.org/10.1086/381298)
- Conselice, C. J., & Gallagher, III, J. S. 1999, *AJ*, 117, 75, doi: [10.1086/300697](https://doi.org/10.1086/300697)
- Conselice, C. J., Yang, C., & Bluck, A. F. L. 2009, *MNRAS*, 394, 1956, doi: [10.1111/j.1365-2966.2009.14396.x](https://doi.org/10.1111/j.1365-2966.2009.14396.x)
- Courtois, H. M., & Tully, R. B. 2015, *MNRAS*, 447, 1531, doi: [10.1093/mnras/stu2405](https://doi.org/10.1093/mnras/stu2405)
- Crnojević, D., Sand, D. J., Caldwell, N., et al. 2014, *ArXiv e-prints*. <https://arxiv.org/abs/1409.4776>
- Duc, P.-A., Paudel, S., McDermid, R. M., et al. 2014a, *MNRAS*, doi: [10.1093/mnras/stu330](https://doi.org/10.1093/mnras/stu330)
- Duc, P.-A., & Renaud, F. 2013, in *Lecture Notes in Physics*, Berlin Springer Verlag, Vol. 861, Lecture Notes in Physics, Berlin Springer Verlag, ed. J. Souchay, S. Mathis, & T. Tokieda, 327
- Duc, P.-A., Cuillandre, J.-C., Serra, P., et al. 2011, *MNRAS*, 417, 863, doi: [10.1111/j.1365-2966.2011.19137.x](https://doi.org/10.1111/j.1365-2966.2011.19137.x)
- Duc, P.-A., Cuillandre, J.-C., Karabal, E., et al. 2014b, *ArXiv e-prints*. <https://arxiv.org/abs/1410.0981>
- . 2015, *MNRAS*, 446, 120, doi: [10.1093/mnras/stu2019](https://doi.org/10.1093/mnras/stu2019)
- Ekta, Chengalur, J. N., & Pustilnik, S. A. 2008, *MNRAS*, 391, 881, doi: [10.1111/j.1365-2966.2008.13928.x](https://doi.org/10.1111/j.1365-2966.2008.13928.x)
- Eneev, T. M., Kozlov, N. N., & Sunyaev, R. A. 1973, *A&A*, 22, 41
- Gallagher, III, J. S., Hunter, D. A., & Tutukov, A. V. 1984, *ApJ*, 284, 544, doi: [10.1086/162437](https://doi.org/10.1086/162437)

- Gallagher, III, J. S., & Parker, A. 2010, *ApJ*, 722, 1962, doi: [10.1088/0004-637X/722/2/1962](https://doi.org/10.1088/0004-637X/722/2/1962)
- Geha, M., Blanton, M. R., Yan, R., & Tinker, J. L. 2012, *ApJ*, 757, 85, doi: [10.1088/0004-637X/757/1/85](https://doi.org/10.1088/0004-637X/757/1/85)
- Geha, M., Guhathakurta, P., & van der Marel, R. P. 2005, *AJ*, 129, 2617, doi: [10.1086/430188](https://doi.org/10.1086/430188)
- Gil de Paz, A., Madore, B. F., & Pevunova, O. 2003, *ApJS*, 147, 29, doi: [10.1086/374737](https://doi.org/10.1086/374737)
- Giovanelli, R., Haynes, M. P., Kent, B. R., et al. 2005, *AJ*, 130, 2598, doi: [10.1086/497431](https://doi.org/10.1086/497431)
- Graham, A. W., Spitler, L. R., Forbes, D. A., et al. 2012, *ApJ*, 750, 121, doi: [10.1088/0004-637X/750/2/121](https://doi.org/10.1088/0004-637X/750/2/121)
- Gwyn, S. D. J. 2008, *PASP*, 120, 212, doi: [10.1086/526794](https://doi.org/10.1086/526794)
- James, B. L., Tsamis, Y. G., Barlow, M. J., Walsh, J. R., & Westmoquette, M. S. 2013, *MNRAS*, 428, 86, doi: [10.1093/mnras/sts004](https://doi.org/10.1093/mnras/sts004)
- Janz, J., & Lisker, T. 2009, *ApJL*, 696, L102, doi: [10.1088/0004-637X/696/1/L102](https://doi.org/10.1088/0004-637X/696/1/L102)
- Johnson, M. 2013, *AJ*, 145, 146, doi: [10.1088/0004-6256/145/6/146](https://doi.org/10.1088/0004-6256/145/6/146)
- Kennicutt, Jr., R. C. 1998, *ARA&A*, 36, 189, doi: [10.1146/annurev.astro.36.1.189](https://doi.org/10.1146/annurev.astro.36.1.189)
- Kim, T., Sheth, K., Hinz, J. L., et al. 2012, *ApJ*, 753, 43, doi: [10.1088/0004-637X/753/1/43](https://doi.org/10.1088/0004-637X/753/1/43)
- Klypin, A., Zhao, H., & Somerville, R. S. 2002, *ApJ*, 573, 597, doi: [10.1086/340656](https://doi.org/10.1086/340656)
- Kormendy, J., Fisher, D. B., Cornell, M. E., & Bender, R. 2009, *ApJS*, 182, 216, doi: [10.1088/0067-0049/182/1/216](https://doi.org/10.1088/0067-0049/182/1/216)
- Lee, J. C., Gil de Paz, A., Tremonti, C., et al. 2009, *ApJ*, 706, 599, doi: [10.1088/0004-637X/706/1/599](https://doi.org/10.1088/0004-637X/706/1/599)
- Lelli, F., Verheijen, M., & Fraternali, F. 2014, *MNRAS*, 445, 1694, doi: [10.1093/mnras/stu1804](https://doi.org/10.1093/mnras/stu1804)
- Leroy, A. K., Walter, F., Brinks, E., et al. 2008, *AJ*, 136, 2782, doi: [10.1088/0004-6256/136/6/2782](https://doi.org/10.1088/0004-6256/136/6/2782)
- Lisker, T. 2009, *Astronomische Nachrichten*, 330, 1043, doi: [10.1002/asna.200911291](https://doi.org/10.1002/asna.200911291)
- Martin, D. C., Fanson, J., Schiminovich, D., et al. 2005, *ApJL*, 619, L1, doi: [10.1086/426387](https://doi.org/10.1086/426387)
- Martínez-Delgado, D., Romanowsky, A. J., Gabany, R. J., et al. 2012, *ApJL*, 748, L24, doi: [10.1088/2041-8205/748/2/L24](https://doi.org/10.1088/2041-8205/748/2/L24)
- Meyer, H. T., Lisker, T., Janz, J., & Papaderos, P. 2014, *A&A*, 562, A49, doi: [10.1051/0004-6361/201220700](https://doi.org/10.1051/0004-6361/201220700)
- Meyer, M. J., Zwaan, M. A., Webster, R. L., et al. 2004, *MNRAS*, 350, 1195, doi: [10.1111/j.1365-2966.2004.07710.x](https://doi.org/10.1111/j.1365-2966.2004.07710.x)
- Mihos, J. C., Harding, P., Feldmeier, J. J., et al. 2017, *ApJ*, 834, 16, doi: [10.3847/1538-4357/834/1/16](https://doi.org/10.3847/1538-4357/834/1/16)
- Naab, T., Johansson, P. H., Ostriker, J. P., & Efstathiou, G. 2007, *ApJ*, 658, 710, doi: [10.1086/510841](https://doi.org/10.1086/510841)
- Nidever, D. L., Ashley, T., Slater, C. T., et al. 2013, *ApJL*, 779, L15, doi: [10.1088/2041-8205/779/2/L15](https://doi.org/10.1088/2041-8205/779/2/L15)
- Papaderos, P., Loose, H.-H., Thuan, T. X., & Fricke, K. J. 1996, *A&AS*, 120, 207
- Patton, D. R., Torrey, P., Ellison, S. L., Mendel, J. T., & Scudder, J. M. 2013, *MNRAS*, 433, L59, doi: [10.1093/mnras/slt058](https://doi.org/10.1093/mnras/slt058)
- Paturel, G., Theureau, G., Bottinelli, L., et al. 2003, *A&A*, 412, 57, doi: [10.1051/0004-6361:20031412](https://doi.org/10.1051/0004-6361:20031412)
- Paudel, S., Duc, P. A., & Ree, C. H. 2015, *AJ*, 149, 114, doi: [10.1088/0004-6256/149/3/114](https://doi.org/10.1088/0004-6256/149/3/114)
- Paudel, S., Lisker, T., Hansson, K. S. A., & Huxor, A. P. 2014, *MNRAS*, 443, 446, doi: [10.1093/mnras/stu1171](https://doi.org/10.1093/mnras/stu1171)
- Paudel, S., & Ree, C. H. 2014, *ArXiv e-prints*, <https://arxiv.org/abs/1410.7848>
- Paudel, S., & Sengupta, C. 2017, *ApJL*, 849, L28, doi: [10.3847/2041-8213/aa95bf](https://doi.org/10.3847/2041-8213/aa95bf)
- Paudel, S., Duc, P.-A., Cote, P., et al. 2013, *ArXiv e-prints*, <https://arxiv.org/abs/1302.6611>
- Paudel, S., Smith, R., Duc, P.-A., et al. 2017, *ApJ*, 834, 66, doi: [10.3847/1538-4357/834/1/66](https://doi.org/10.3847/1538-4357/834/1/66)
- Pearson, S., Besla, G., Putman, M. E., et al. 2016, *MNRAS*, 459, 1827, doi: [10.1093/mnras/stw757](https://doi.org/10.1093/mnras/stw757)
- Privon, G. C., Stierwalt, S., Patton, D. R., et al. 2017, *ApJ*, 846, 74, doi: [10.3847/1538-4357/aa8560](https://doi.org/10.3847/1538-4357/aa8560)
- Putman, M. E., Staveley-Smith, L., Freeman, K. C., Gibson, B. K., & Barnes, D. G. 2003, *ApJ*, 586, 170, doi: [10.1086/344477](https://doi.org/10.1086/344477)
- Rhee, J., Smith, R., Choi, H., et al. 2017, *ApJ*, 843, 128, doi: [10.3847/1538-4357/aa6d6c](https://doi.org/10.3847/1538-4357/aa6d6c)
- Rich, R. M., Collins, M. L. M., Black, C. M., et al. 2012, *Nature*, 482, 192, doi: [10.1038/nature10837](https://doi.org/10.1038/nature10837)
- Schlafly, E. F., & Finkbeiner, D. P. 2011, *ApJ*, 737, 103, doi: [10.1088/0004-637X/737/2/103](https://doi.org/10.1088/0004-637X/737/2/103)
- Sengupta, C., Scott, T. C., Dwarakanath, K. S., Saikia, D. J., & Sohn, B. W. 2014, *MNRAS*, 444, 558, doi: [10.1093/mnras/stu1463](https://doi.org/10.1093/mnras/stu1463)
- Sengupta, C., Scott, T. C., Verdes Montenegro, L., et al. 2012, *A&A*, 546, A95, doi: [10.1051/0004-6361/201219948](https://doi.org/10.1051/0004-6361/201219948)
- Smith, B. J., Struck, C., Hancock, M., et al. 2007, *AJ*, 133, 791, doi: [10.1086/510350](https://doi.org/10.1086/510350)
- Spergel, D. N., Bean, R., Doré, O., et al. 2007, *ApJS*, 170, 377, doi: [10.1086/513700](https://doi.org/10.1086/513700)
- Springel, V., White, S. D. M., Jenkins, A., et al. 2005, *Nature*, 435, 629, doi: [10.1038/nature03597](https://doi.org/10.1038/nature03597)
- Stierwalt, S., Besla, G., Patton, D., et al. 2015, *ApJ*, 805, 2, doi: [10.1088/0004-637X/805/1/2](https://doi.org/10.1088/0004-637X/805/1/2)
- Struck, C. 1999, *PhR*, 321, 1, doi: [10.1016/S0370-1573\(99\)00030-7](https://doi.org/10.1016/S0370-1573(99)00030-7)

- Struck, C., & Smith, B. J. 2012, MNRAS, 422, 2444,
doi: [10.1111/j.1365-2966.2012.20798.x](https://doi.org/10.1111/j.1365-2966.2012.20798.x)
- Tal, T., van Dokkum, P. G., Nelan, J., & Bezanson, R.
2009, AJ, 138, 1417, doi: [10.1088/0004-6256/138/5/1417](https://doi.org/10.1088/0004-6256/138/5/1417)
- Toloba, E., Guhathakurta, P., van de Ven, G., et al. 2014,
ApJ, 783, 120, doi: [10.1088/0004-637X/783/2/120](https://doi.org/10.1088/0004-637X/783/2/120)
- Toomre, A., & Toomre, J. 1972, ApJ, 178, 623,
doi: [10.1086/151823](https://doi.org/10.1086/151823)
- van Dokkum, P. G. 2005, AJ, 130, 2647,
doi: [10.1086/497593](https://doi.org/10.1086/497593)
- Yozin, C., & Bekki, K. 2012, ApJL, 756, L18,
doi: [10.1088/2041-8205/756/1/L18](https://doi.org/10.1088/2041-8205/756/1/L18)

APPENDIX

A. NOTES ON SELECTED INDIVIDUAL SYSTEM

In this Section, we provide a short list of previously published studies on individual objects in our sample. We note that the list is not complete or fully comprehensive, but we hope it provides a useful starting point for readers with an interest in a specific object or merging system.

Id01130052: A gas rich low metallicity dwarf galaxy, [Ekta et al. \(2008\)](#) find disturbed HI velocity field and suggest ongoing merger.

Id0202-0922: Dwarf antennae system produced by merging two gas-rich dwarf galaxies. A detail study of of the system from HI data has been submitted for the publication, Paudel et al.

Id02032202: This galaxy is located in isolation and [Sengupta et al. \(2012\)](#) reported ongoing minor merger in this galaxy. They detected an a symmetry feature in HI map.

Id0851-0221: ARP 257: from catalog of interacting galaxies ([Arp 1966](#))

Id08580619: Interacting dwarf pair in the vicinity of an isolated spiral galaxy NGC 2718. [Paudel & Sengupta \(2017\)](#) reported the system as LMC-SMC-MW analoge.

Id09003543: Arp 202: from catalog of interacting galaxies. A detail study of the system has been performed in [Sengupta et al. \(2014\)](#) and they reported formation of tidal dwarf galaxies of stellar mass $2 \times 10^8 M_{\odot}$.

Id09002536: An isolated galaxy. [Chengalur et al. \(2015\)](#) identified a disturbed HI morphology and argued that the galaxy has suffered recent minor merger.

Id09562849: A merging dwarf candidate [Annibali et al. \(2016\)](#)

Id10080227: A merger origin compact early-type galaxy ([Paudel et al. 2014](#))

Id10545418: Interacting pair studied in Local Volume TiNy Titan ([Pearson et al. 2016](#))

Id11451711: Interacting dwarf galaxies in the outskirts of a group environment ([Paudel et al. 2013](#)).

Id1148-0138: [Lelli et al. \(2014\)](#) studied this galaxy and concluded that star-formation rate is enhanced due to merger/interaction in recent past.

Id12250548: VCC848, a merging Blue Compact Dwarf in Virgo cluster.

Id12284405: NGC 4449: Interacting dwarf galaxies reported by ([Martínez-Delgado et al. 2012](#); [Rich et al. 2012](#))

Id12304138: Interacting pair studied in Local Volume TiNy Titan ([Pearson et al. 2016](#))

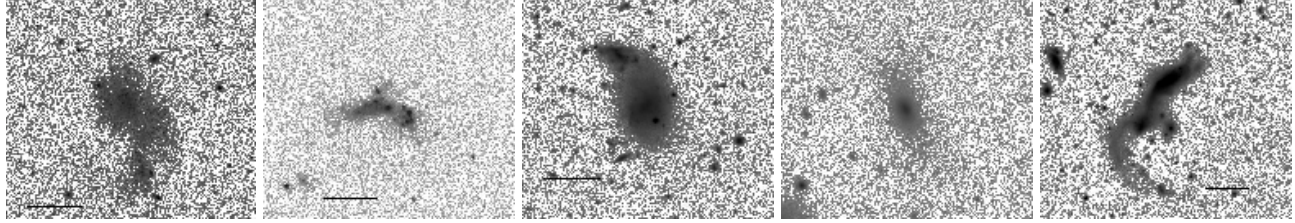
Id12474709: ARP 277

Id14503534: Interacting pair studied in Local Volume TiNy Titan ([Pearson et al. 2016](#))

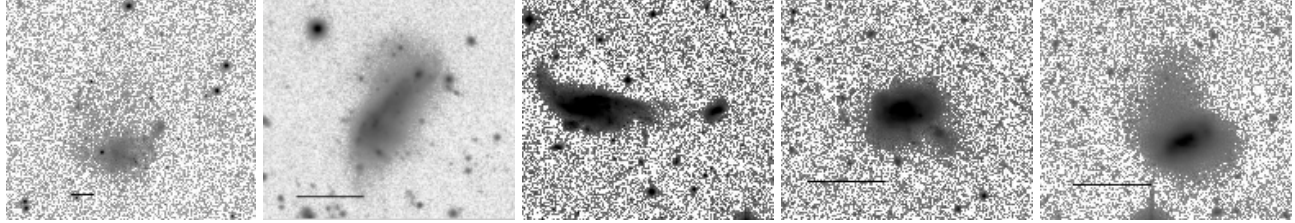
Id14503534: Part of TiNy Titan, dwarf interacting pair studied in [Privon et al. \(2017\)](#).

B. FIGURE CATALOG

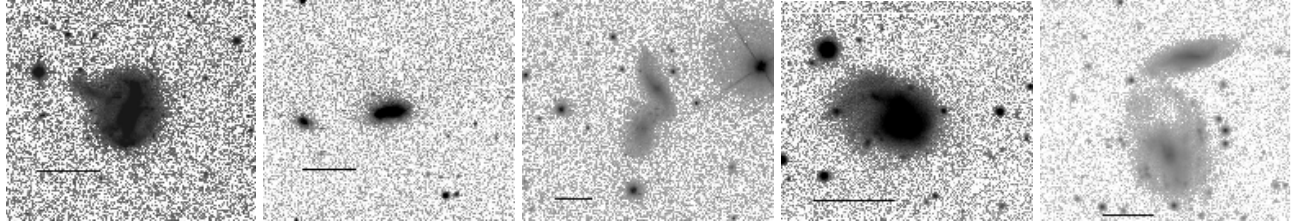
001 to 005



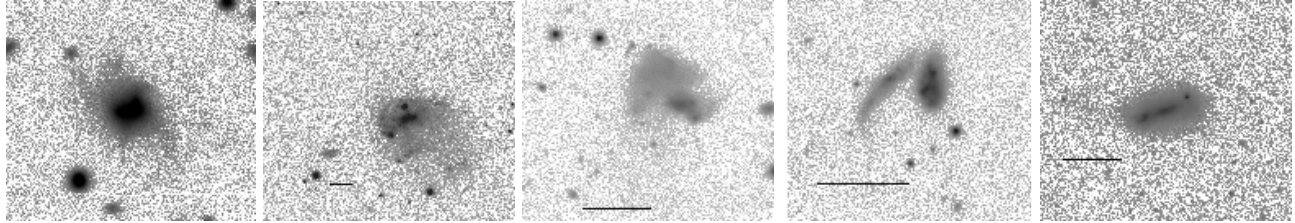
006 to 010



011 to 015



016 to 020



021 to 025

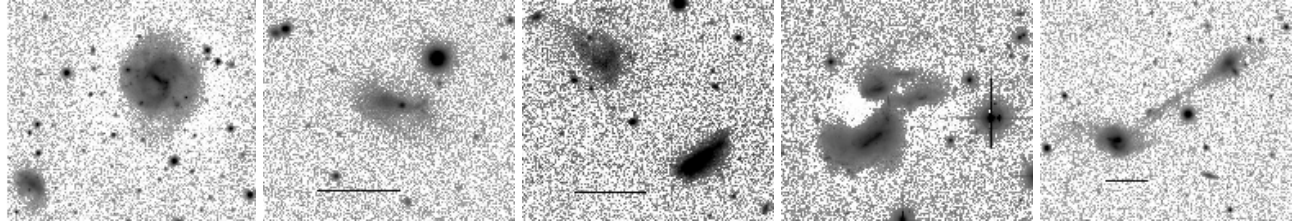
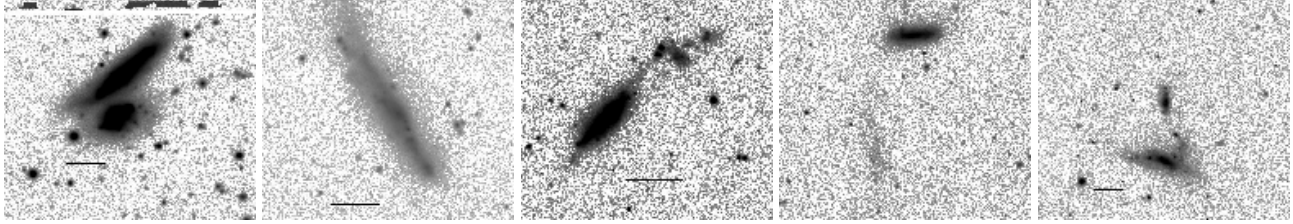
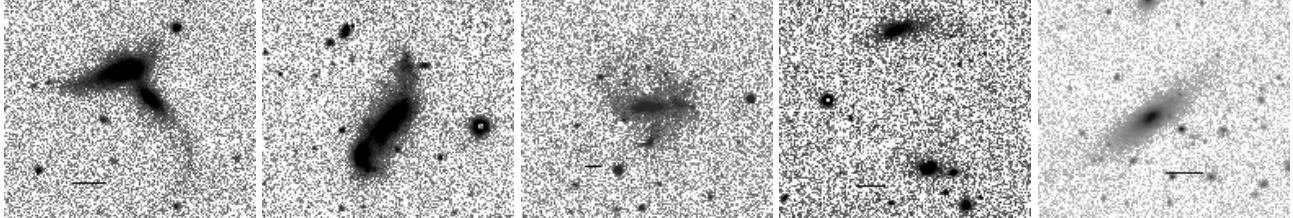


Figure 12. These postage images are prepared from fits images downloaded from various archive. On the top of each row, we list identification of these galaxies according to Table 1. The field of view and color stretching is arbitrarily chosen to make best view of both interacting galaxies and low-surface brightness features. An image scale of $30''$ is shown by the black horizontal bar.

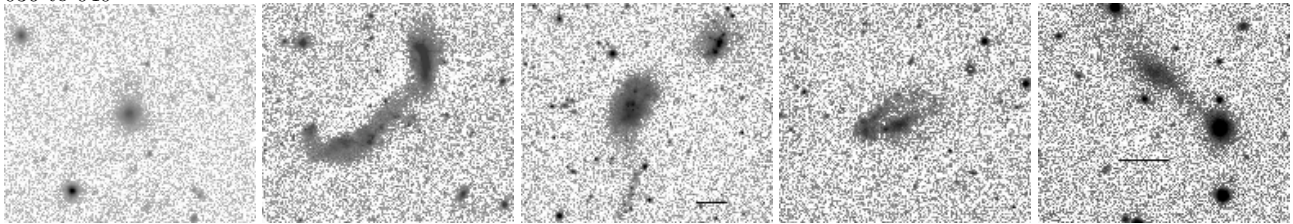
026 to 030



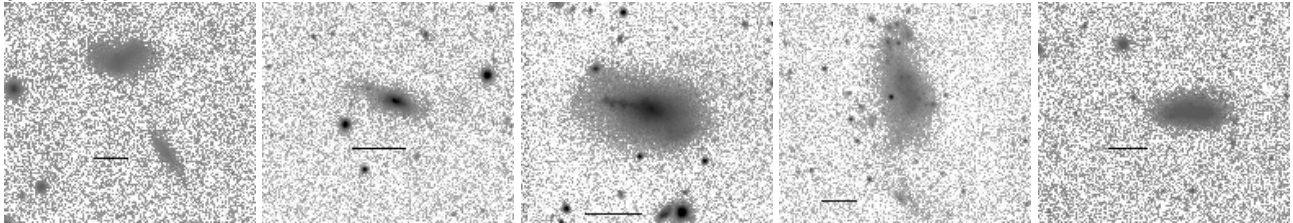
031 to 035



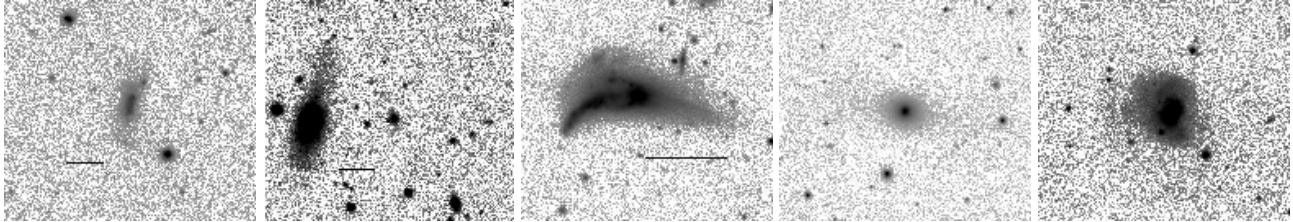
036 to 040



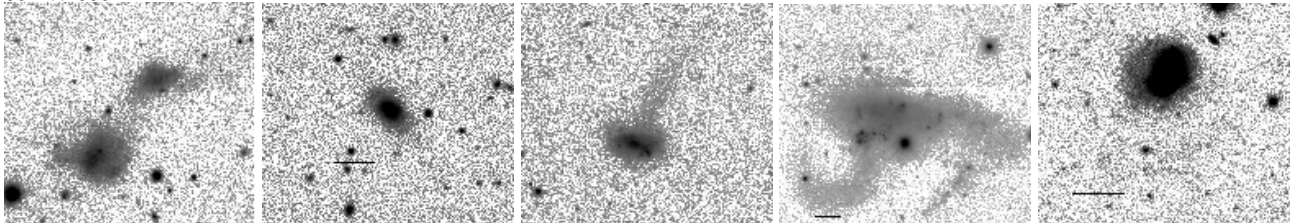
041 to 045



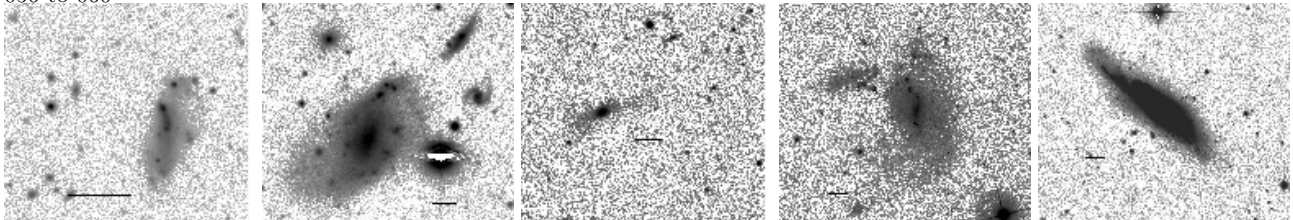
046 to 050



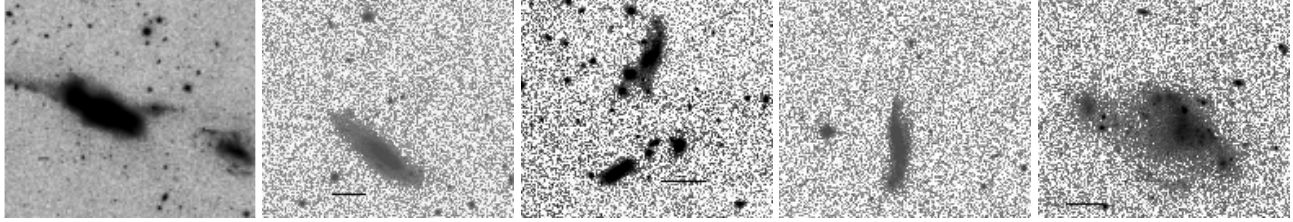
051 to 055



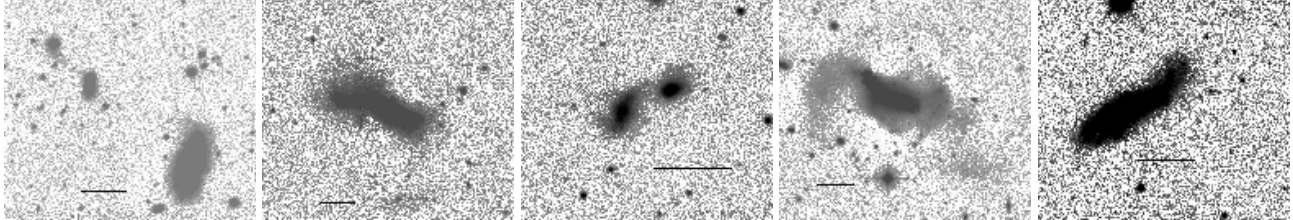
056 to 060



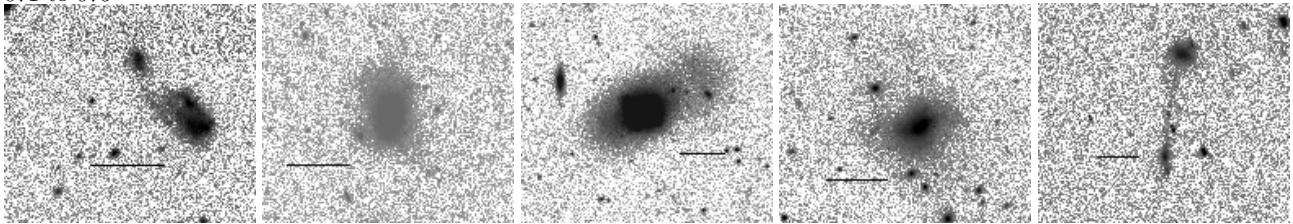
061 to 065



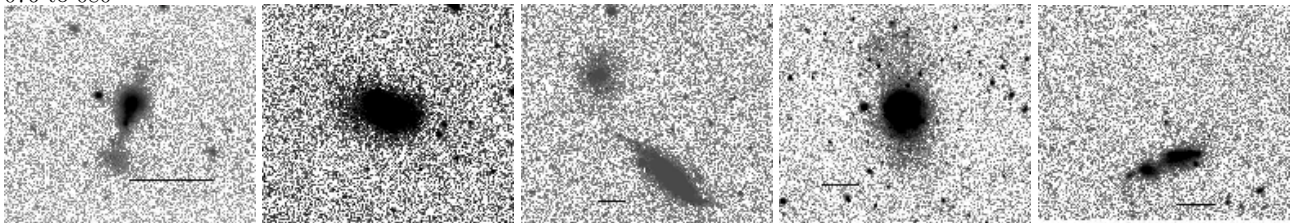
066 to 070



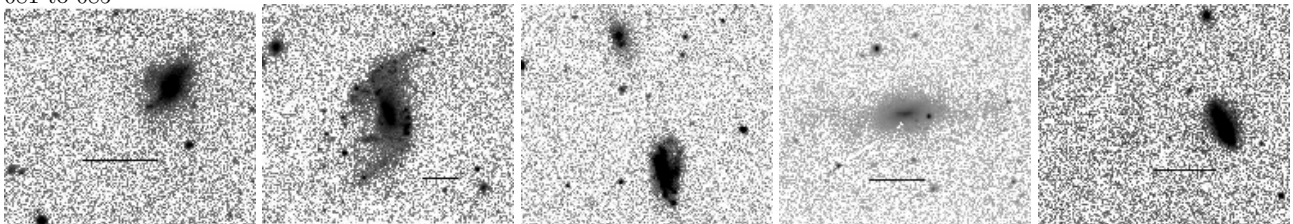
071 to 075



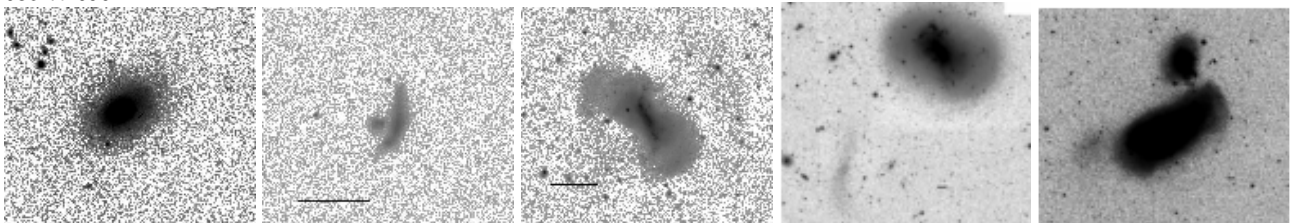
076 to 080



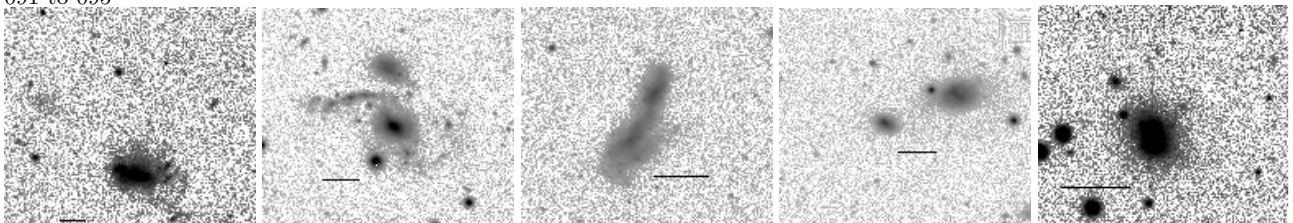
081 to 085



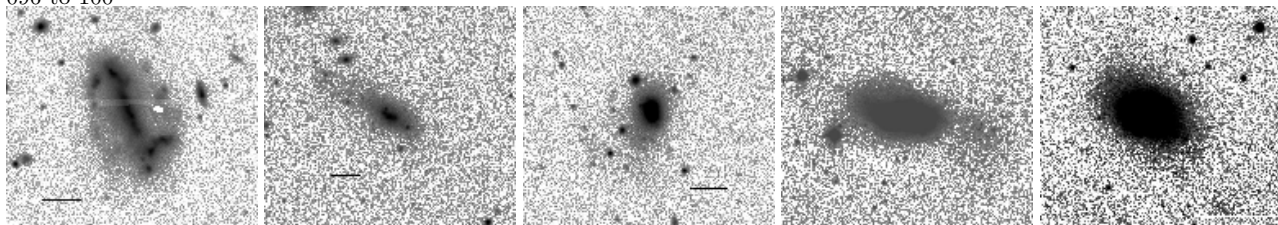
086 to 090



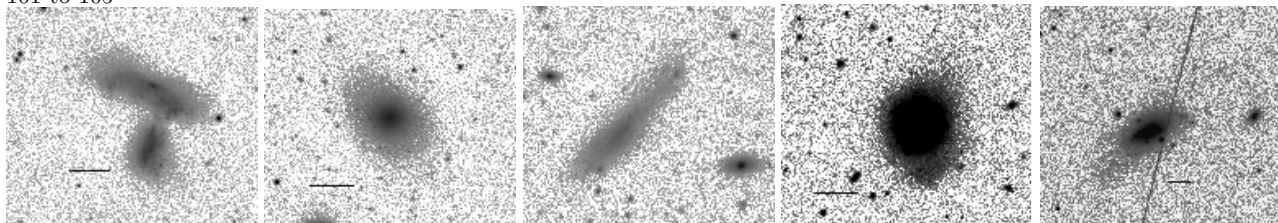
091 to 095



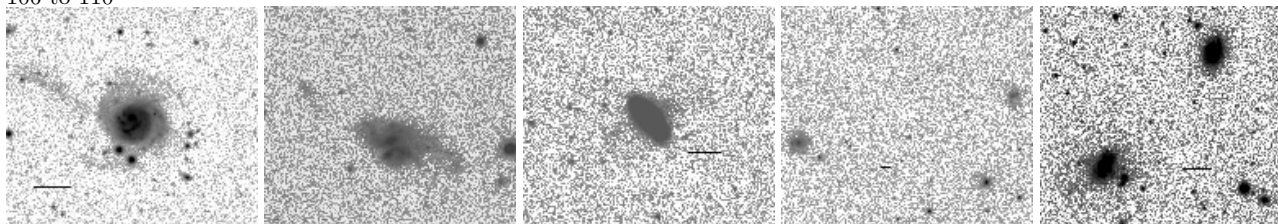
096 to 100



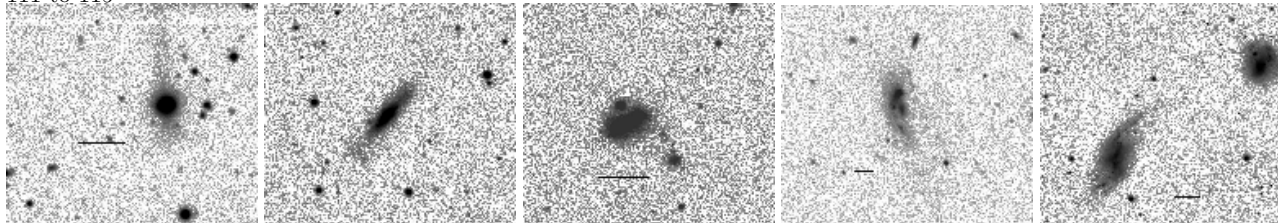
101 to 105



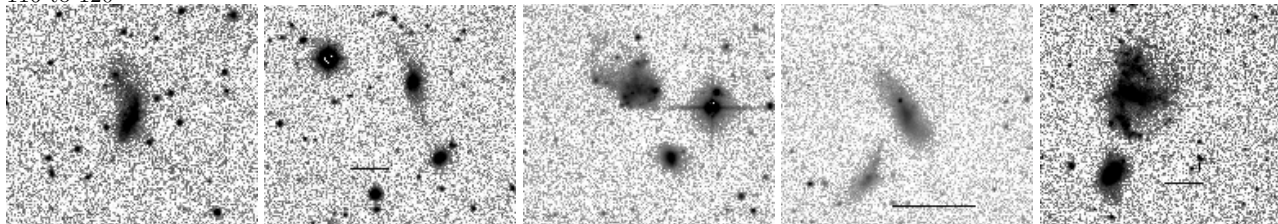
106 to 110



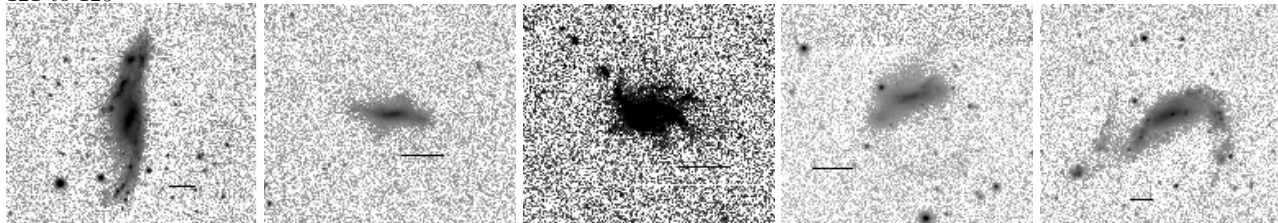
111 to 115



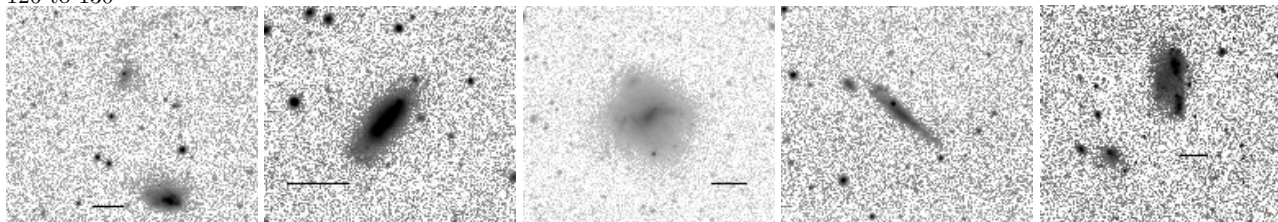
116 to 120



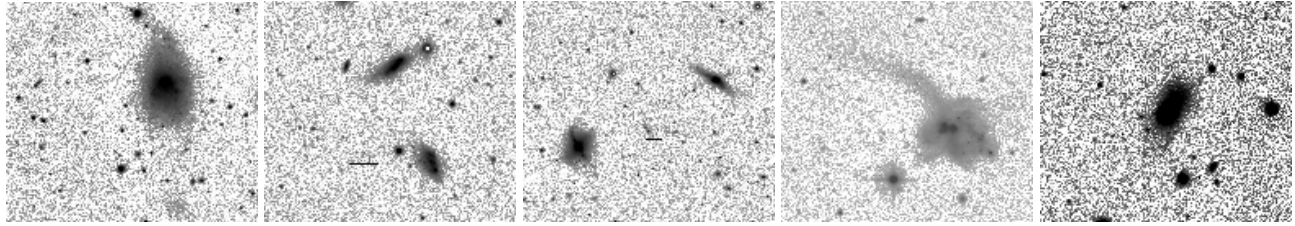
121 to 125



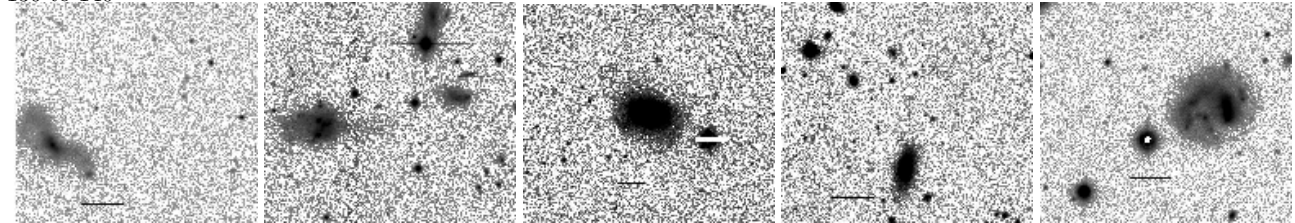
126 to 130



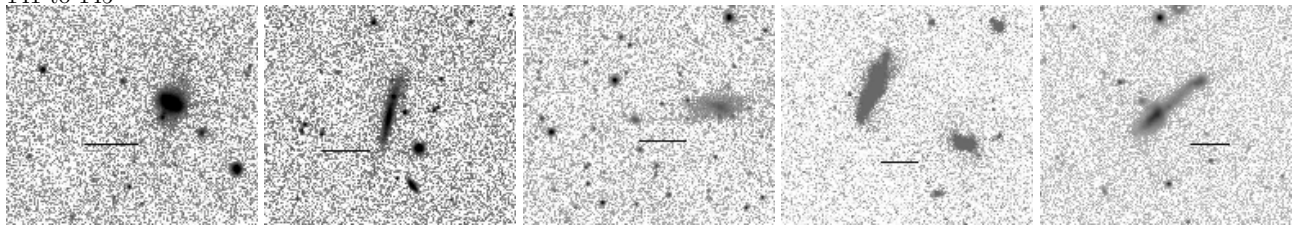
131 to 135



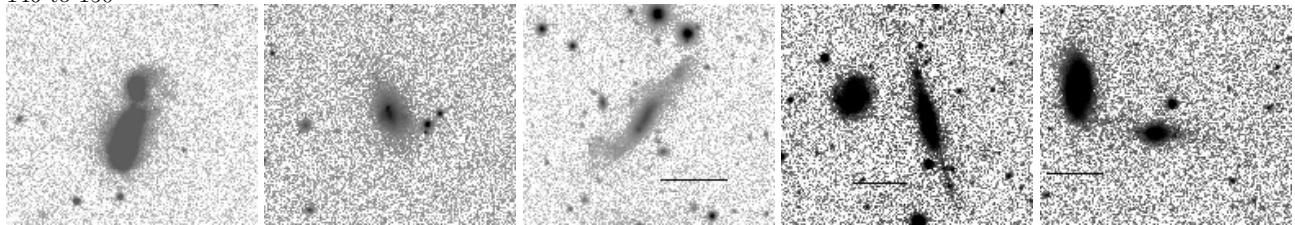
136 to 140



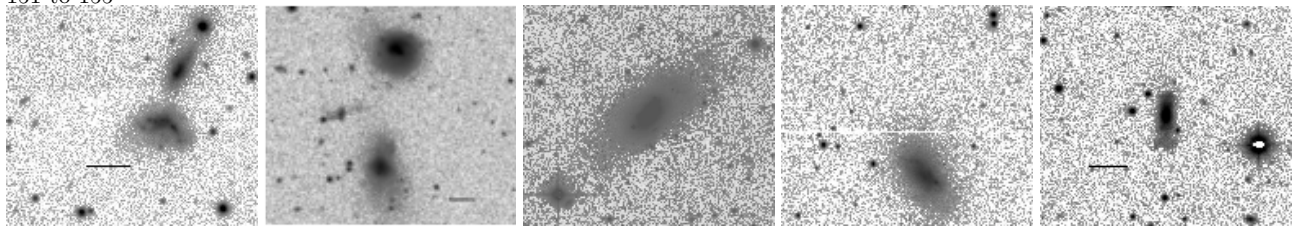
141 to 145



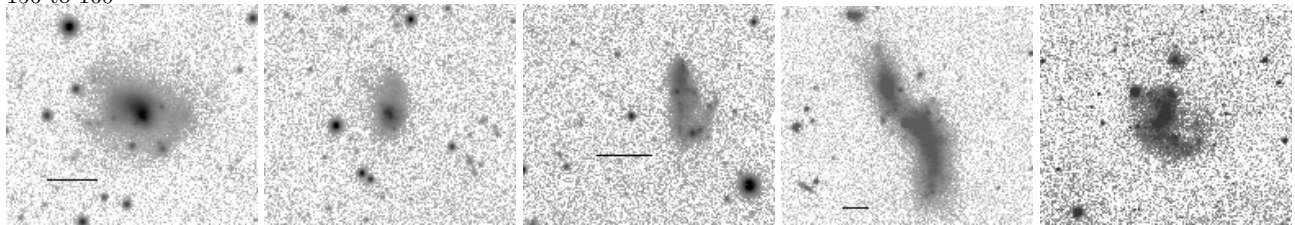
146 to 150



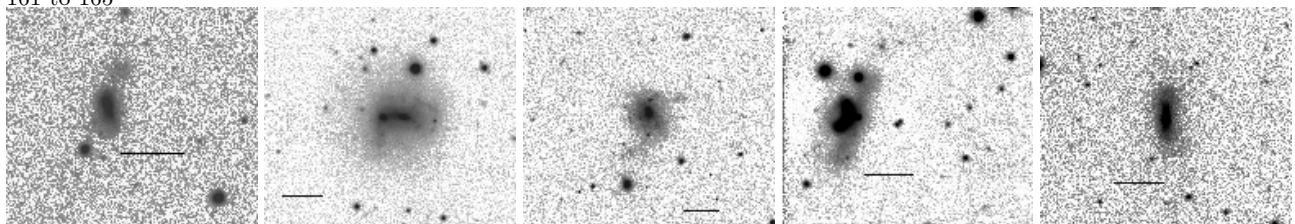
151 to 155



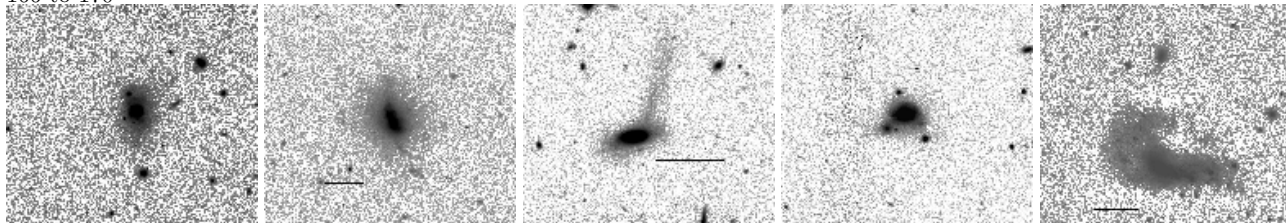
156 to 160



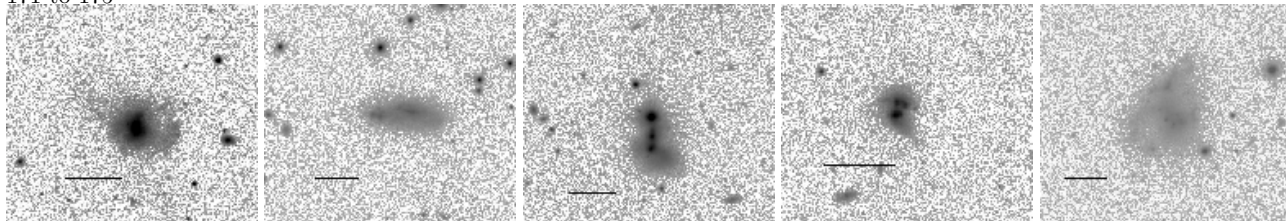
161 to 165



166 to 170



171 to 175



176 to 177

